

## **Master thesis : Design of a System to Investigate Underwater Radiated Noise of Small Craft**

**Auteur :** Berrio Barrera, Carlos Javier

**Promoteur(s) :** 14957

**Faculté :** Faculté des Sciences appliquées

**Diplôme :** Master : ingénieur civil mécanicien, à finalité spécialisée en "Advanced Ship Design"

**Année académique :** 2021-2022

**URI/URL :** <http://hdl.handle.net/2268.2/16558>

---

### *Avertissement à l'attention des usagers :*

*Tous les documents placés en accès ouvert sur le site le site MatheO sont protégés par le droit d'auteur. Conformément aux principes énoncés par la "Budapest Open Access Initiative"(BOAI, 2002), l'utilisateur du site peut lire, télécharger, copier, transmettre, imprimer, chercher ou faire un lien vers le texte intégral de ces documents, les disséquer pour les indexer, s'en servir de données pour un logiciel, ou s'en servir à toute autre fin légale (ou prévue par la réglementation relative au droit d'auteur). Toute utilisation du document à des fins commerciales est strictement interdite.*

*Par ailleurs, l'utilisateur s'engage à respecter les droits moraux de l'auteur, principalement le droit à l'intégrité de l'oeuvre et le droit de paternité et ce dans toute utilisation que l'utilisateur entreprend. Ainsi, à titre d'exemple, lorsqu'il reproduira un document par extrait ou dans son intégralité, l'utilisateur citera de manière complète les sources telles que mentionnées ci-dessus. Toute utilisation non explicitement autorisée ci-avant (telle que par exemple, la modification du document ou son résumé) nécessite l'autorisation préalable et expresse des auteurs ou de leurs ayants droit.*

---



With the support of the  
Erasmus+ Programme  
of the European Union

**DW**  
SHIPCONSULT

# Design of a System to Investigate Underwater Radiated Noise of Small Craft

submitted on 29<sup>th</sup> July 2022

by

BERRIO BARRERA Carlos Javier | Klein-Ebbenkamp 1 | 24149 Kiel | carlos.barrera@uni-rostock.de

Student ID No.: 221 200 011

**First Reviewer:**

Prof. Dr. Eng. Patrick Kaeding

Chair of Ship Structures

University of Rostock Albert-Einstein-Str. 2

18059 Rostock

Germany

**Second Reviewer:**

Dr.-Ing. Dietrich Wittekind

Managing Director

DW-ShipConsult GmbH Lise-Meitner-Str. 9

24223 Schwentinental

Germany

# CONTENTS

LIST OF FIGURES.....	iv
LIST OF TABLES .....	vi
LIST OF SYMBOLS .....	vii
LIST OF ABBREVIATIONS .....	viii
DECLARATION OF AUTHORSHIP .....	ix
ABSTRACT .....	x
1 INTRODUCTION.....	1
1.1. Underwater Noise Measurement. Background.....	2
1.2. Scope .....	3
2. THEORETICAL FRAMEWORK .....	4
2.1. Underwater Noise .....	4
2.1.1. Sound Propagation .....	5
2.1.1.1. Acoustic Pressure.....	6
2.1.1.2. Propagation Speed .....	6
2.2. Underwater Noise Measurement .....	7
2.2.1. Measurement Parameters .....	8
2.2.1.1. Wave Pressure Amplitude.....	8
2.2.1.2. Wave Pressure Frequency .....	8
2.2.1.3. Pressure Wave Period .....	9
2.2.1.4. Wavelength .....	9
2.2.1.5. Phase .....	10
2.2.1.6. Sample Frequency.....	10
2.2.1.7. Design Frequency .....	10
2.2.2. Signal Processing .....	10
2.2.2.1. Band Filter .....	11
2.2.2.2. Octave Band.....	11
2.2.2.3. Spectrogram .....	11
2.2.3. Sound Pressure Level .....	12
2.2.3.1. Signal to Noise Ratio .....	13
2.3. Underwater Radiated Noise of Recreational Craft .....	14
2.4. Sound Detection .....	15
2.5. Sound Bearing and Localization Methods.....	15

2.5.1.	Received Signal Strength .....	15
2.5.2.	Time of Arrival.....	16
2.5.3.	DOA & TDOA Principles .....	18
2.5.3.1.	2-Hydrophones Array .....	18
2.5.3.2.	3-Hydrophones Array .....	19
2.6.	Cross-Correlation Function .....	22
3.	METHODOLOGY .....	25
3.1.	Validation DOA Model with a 2-Microphones Linear Array .....	25
3.2.	4-Hydrophones Planar Array Design Stage.....	34
3.3.	4-Hydrophones Planar Squared Array Building Stage.....	38
3.4.	4-Hydrophones Planar Squared Array Testing Stage.....	39
4.	RESULTS AND ANALYSIS .....	42
4.1.	Acoustic Data Processing .....	42
4.2.	Bearing Calculations.....	46
5.	CONCLUSIONS .....	57
6.	ACKNOWLEDGEMENTS .....	59
7.	REFERENCES.....	60

## LIST OF FIGURES

Figure 1. Representation of the refraction of a sound wave in seawater .....	5
Figure 2. Acoustic signal basic parameters .....	9
Figure 3. a) Two sinusoidal signals with frequency variation in time. b) Frequency spectrum of both signals. c) Spectrogram of signal 1 (up) d) Spectrogram of signal 2 (down) .....	12
Figure 4. Estimated number of recreational boats owned. (McCarthy, 2004) .....	14
Figure 5. TOA approach with three receivers to locate a source .....	17
Figure 6. 2-hydrophones linear array .....	18
Figure 7. 3-hydrophones planar array (DOA) .....	19
Figure 8. 3-hydrophones planar array (TDOA) .....	21
Figure 9. Sinusoidal signals delayed each other .....	23
Figure 10. Signals from two hydrophones in a linear array .....	23
Figure 11. Cross-correlation steps of a simple wave signal .....	24
Figure 12. Source positions .....	26
Figure 13. B&K-PCB Microphone linear array .....	26
Figure 14. Recording of microphones of 1 kHz signal at P <sub>4</sub> .....	27
Figure 15. Octave spectrum of 1 kHz at P <sub>4</sub> .....	28
Figure 16. Recording of microphones of motor boat at P <sub>4</sub> .....	28
Figure 17. Octave spectrum of motor boat at P <sub>4</sub> .....	29
Figure 18. Octave spectrum of 1 kHz sinusoidal .....	29
Figure 19. Octave spectrum of motor boat signal .....	30
Figure 20. Cross-correlation function .....	31
Figure 21. Cross-correlation peaks function .....	31
Figure 22. Bearing of sinusoidal wave signal .....	32
Figure 23. Bearing ship signal.....	33
Figure 24. Modeling of hydrophone .....	34
Figure 25. a) Triangular array. Proposal design 1. b) Horizontal Squared Array. Proposal design 2. ....	35
Figure 26. Proposal 1 sketch .....	36
Figure 27. Proposal 2 sketch .....	37
Figure 28. Final proposal for measurement design .....	38
Figure 29. Array Assembled .....	40
Figure 30. Deployment scheme.....	40

Figure 31. Compass for reference angle (left) and deployment of the array .....	41
Figure 32. Sailing route description .....	41
Figure 33. Maritime route of two big ships in recording zone .....	42
Figure 34. Background noise sample .....	43
Figure 35. Recorded time spectrogram .....	44
Figure 36. Identification of sources in spectrogram .....	45
Figure 37. DOA model algorithm scheme .....	46
Figure 38. Histogram of SNR values per hydrophone .....	47
Figure 39. Cross-correlation function. a) Hydrophones A-B, b) Hydrophones A-C and c) Hydrophones A-D .....	48
Figure 40. Estimated bearing (azimuth) compared to GPS data .....	48
Figure 41. Separation distance array-Sailing boat in time .....	49
Figure 42. Bearing error histogram Section I .....	49
Figure 43. Bearing error histograms of section II (left) & section III (right) .....	50
Figure 44. Bearing error histograms of section IV (left) & section VI (right) .....	50
Figure 45. Bearing error histogram of section VII (left) & section VIII (right) .....	51
Figure 46. Bearing error histogram of section IX (left) & section X (right) .....	52
Figure 47. Overall bearing error histogram .....	52
Figure 48. Bearing reference to recording zone .....	54
Figure 49. One-Third octave spectrum (Sailing boat) .....	55
Figure 50. One-Third octave spectrum (fast boat, Ferry and Sailing boat) .....	55
Figure 51. One-Third octave spectrum (SFK Ferry) .....	56

## LIST OF TABLES

Table 1. Comparison of passive sound localization methods .....	22
Table 2. Recording system specification two hydrophones linear array.....	25
Table 3. Condition and specification of the linear array .....	26
Table 4. Bearing from 1 kHz Sinusoidal wave signal.....	32
Table 5. Bearing from Motor boat signal .....	33
Table 6. Array design decision matrix .....	37
Table 7. Material list for the array construction.....	39
Table 8. List of ships registered during the experiment.....	53

## LIST OF SYMBOLS

$C$	Propagation speed
$\mathbf{s}$	Position vector to the source
$\mathbf{m}_i$	Position vector to the receptor $i$
$\tau$	Time delay
$A_{RMS}$	Root mean square amplitude
$f$	Frequency
$f_s$	Sampling frequency
$\lambda$	Wavelength
$\phi$	Phase



## LIST OF ABBREVIATIONS

DOA	Direction of Arrival
SNR	Sound to Noise Ratio
SPL	Sound Pressure Level
URN	Underwater Radiated Noise
TDOA	Time Delay of Arrival
TOA	Time of Arrival
RSS	Received Strength Signal
CET	Central European Time
GPS	Global Positioning System

## **DECLARATION OF AUTHORSHIP**

I declare that this thesis and the work presented in it are my own and have been generated by me as the result of my own original research.

Where I have consulted the published work of others, this is always clearly attributed.

Where I have quoted from the work of others, the source is always given. With the exception of such quotations, this thesis is entirely my own work.

I have acknowledged all main sources of help.

Where the thesis is based on work done by myself jointly with others, I have made clear exactly what was done by others and what I have contributed myself.

This thesis contains no material that has been submitted previously, in whole or in part, for the award of any other academic degree or diploma.

I cede copyright of the thesis in favour of the University of Rostock.

Date: 29<sup>th</sup> July 2022

Signature:

A handwritten signature in black ink, consisting of a stylized 'J' followed by a series of loops and a long horizontal stroke extending to the right.

## ABSTRACT

Underwater Radiated Noise started to be recognized as a threat to the marine ecosystem balance about 50 years ago. Since then, regulations and evaluations of the acoustic signature of big-sized ships have become a common practice. Nowadays, the detection, localization, tracking, and classification of this kind of ship are accurately estimated by radar or AIS. However, in recent years the number of small and mid-sized ships has been increasing rapidly along with human recreational activities in coastal zones, and now is required a better understanding of their environmental impact. Small craft are challenging to detect because of lack of AIS and they have weak acoustic signatures for the most common monitoring systems. Moreover, information published in the literature about the acoustics of this kind of ship is limited, even though they can be widely diverse. This work describes the methodology to design a system to investigate underwater-radiated noise of small craft using only acoustic means. At first, a Direction of Arrival (DOA) model considering two, three and four receivers was formulated and validated. Second, a 4-hydrophones array measurement system was designed, assembled and tested in the bay of Kiel, recording sample data from a motor sailing boat and other vessels passing nearby. Then, the data was processed and evaluated with the DOA model to estimate the bearing location of the recorded sources. Finally, the results were compared with the GPS data from the ships. The system shall then be able to detect the presence of several small craft to later allow entering this information into soundscape calculations.

Keywords: Small craft, DOA, Underwater Radiated Noise.

# 1 INTRODUCTION

Oceans and seas have an important role in Earth's life development. 70% of the planet's surface is occupied by water and around 40% of the world's human population lives in coastal regions (Nations, 2022), and with the rapid increase of industrialization, is not surprising an increase in the degradation of resources in these areas.

Oceans are well known for their huge importance as a source of food supply; about 90% of goods transportation is carried out through ocean environments (OECD, 2022), besides it cannot be ignored the minerals and energy resources located in offshore areas. Nowadays, human impact in marine ecosystem is evident (e.g., microplastic concentration, oil and harmful substances leaks, ship traffic, etc.). Considering the marine environmental balance importance for humans in both, direct and indirect ways, measurements, evaluations and regulations are needed to be established. Over the last 50 years, many agreements and initiatives (e.g. (IMO, 1973), (IMO, 1974), (UN, 1982), (European Commssion, 2008), etc.) have been approved to maintain safe the marine ecosystem condition from known threats, and relatively new ones, such as underwater radiated noise, unnoticed and poorly understood until most recent years. Currently, human-made underwater noise impact is being studied with particular concern to understand deeply noise pollution impact.

Since authorities agreed to understand better oceans, many studies have focused on underwater radiated noise from large ships in open and coastal waters, although, considering that only 1% of biomass is located in open oceans, coastal zones are of essential importance for the world aquatic ecosystem. Hydroacoustics impact in coastal zones has increased considerably in the last two decades, along with the increase of small and mid-sized craft in these areas. Unfortunately, even now it is a matter of concern that marine life is being affected, is not completely clear at which scale. Moreover, small craft are also used in illegal fishing and piracy due to their weak acoustic signals than make them harder to detect with standards monitoring systems and increase the difficulties to study them with more detail.

For social, economic and environmental reasons, coastal zones must be under constant monitoring. For instance, the Marine Strategy Framework Directive (MSFD) (European Commssion, 2008), within their strategy stages, established mandatory measurements, data collection and monitoring programs to each member state in their respective waters. Nevertheless, in practice, a monitoring system for underwater-radiated noise requires not only

accurate measurement instruments but also it must be considered measuring ranges and suitable signal processing techniques.

### **1.1. Underwater Noise Measurement. Background**

Electroacoustic began to develop more than 200 years ago with the observation of mechanical effects in electricity and magnetism. The first direct measurement of the speed of sound in freshwater was made in 1826 in Switzerland (Beyer, 1999), that consisted in striking a submerged bell while at the same time it was flashed a light with an observer kilometers away, measuring the difference between the flash and the sound arrival. This experiment got a value of 1438 m/s, clearly accurate in comparison with the obtained with modern instrumentation (1439 m/s).

In 1880, piezoelectricity was discovered (Hunt, 1954), and years later the bases to develop underwater transducers were established. Nowadays, most of underwater measure instruments are based on them. During World War I, sound waves became more important, because they were the only available mean for signaling through water, as a result, the interest to improve transducers jumped up. Detection and localization of sources at sea are difficult because of background noise, bandwidth limitations, instrumentation range, and more, which make monitoring applications a complex matter. Today, hydrophones are the most common device in hydroacoustics (Arshad, 2009).

In 1994, (Nehorai & Paldi, 1994) proposed a localization technique using sensor arrays to estimate the performance and error in the direction of arrival of a source. The authors proposed two different approaches that eventually led to the direction of arrival method (DOA), one based on vector analysis relating intensity and velocity of signals, and another one by finding the velocity in the source direction.

Since then, several studies have been focused on detection of sources in water through different methods, although, in most of the cases, tracking and constant monitoring were not taken into account. (Xerri, et al., 2000), focused on continuously tracking of a source through a hydrophones array spatially fixed, detecting several time delays of arrivals, making possible the continuous detection of a source on the water surface. This research also introduced the cross-correlation function as a common tool to obtain time delays, highly used in direction of the arrival of models.

Nowadays, DOA-based methods are common in detecting and bearing localization practices, in military, commercial and research fields, regarding not only ships but also marine living beings. Since 2004, AIS system became a common device in every big ship, which eased the detection and tracking in maritime harbors (Marine Traffic). However, small craft does not use this kind of technology (Hermannsen, et al., 2019), therefore new monitoring systems are required. (Tessei, et al., 2011), proposed a system for this kind of ship in shallow water, using tetrahedral arrays placed on the seabed.

This project presents a methodology to design a system to investigate the underwater-radiated noise from small crafts using a 4-hydrophones array as part of a DW-ShipConsult project in partnership with *Deutsches Meeresmuseum Stralsund* and the University of Rostock.

Chapter 2 describes a general overview of underwater acoustic, measurement technology and signal processing techniques. Later on, it is carried out a theoretical review of the main concepts of underwater-radiated noise, formulations of some localization and bearing methods and the model selection for the calculation in the proposed system. Chapter 3, details the methodology to design the proposed measurement system as well as its respective validation. In chapter 4, results provided by the 4-hydrophones array are analyzed and discussed. Finally, chapter 5 points out the conclusions and recommendations for future works related to this topic.

## 1.2. Scope

Based on the statement described previously, the main objective of this project is:

- Design of a system to investigate underwater-radiated noise of small crafts, to detect and bearing locate small craft.

To fulfill the requirement of the main objective of this research, it is expected to:

- Propose a suitable hydrophone array to measure the small craft radiated noise signal.
- Develop a routine to process effectively signals recorded through hydrophone array.
- Validate the signal processing routine for different cases.
- Test the proposed measurement system under real conditions.

## 2. THEORETICAL FRAMEWORK

This chapter offers a brief description of the underwater noise principles, basic definitions of hydroacoustics measurements and signal processing techniques as well as an introduction and formulation of some detection and localization techniques considered for the system design.

### 2.1. Underwater Noise

Sound is a disturbance in pressure caused when an object vibrates. This disturbance propagates through a medium producing compression and tension in the local molecules, transmitting energy but no mass, hence acoustic waves are generated (Kinsler, et al., 2011). Sound and noise are highly related and only distinguished by the listener. In a general aspect, noise is an unwanted sound that interferes with the normal functioning of a system. For instance, when a person uses the word noise, usually it refers to sounds that are annoying enough to interfere with activities such as conversations, thinking, or even sleeping.

Noise is a complex phenomenon, widely studied and still, there is too much to learn about it, but it must be clear that even if it is through air, water, or another propagation medium, noise is something unavoidable. (Ross, 1922), made an analogy between heat and sound; according to the Second Law of Thermodynamics, if heat were not produced in a mechanical process, it would be possible to create a perpetual motion machine. Similarly, every useful mechanical process occurs with some vibration, therefore some level of noise.

While noise power radiated into air varies from the order of microwatts to Megawatts, although power levels in water tend to be from the order of milliwatts (submarines) to kilowatts (ships) (Wittekind, 2017). However, even power levels radiated into water are low in comparison to the radiated in air, underwater noise has many applications. Depending on the field, underwater noise can be measured, reduced or used, for common practices such as:

- Navigation (Autonomous vehicles, depth sounders).
- Asset protection (Harbors).
- Communication (Data).
- Passive monitoring (Ship underwater-radiated noise).
- Research (Biologic, oceanographic, offshore exploration).

In common scenarios, underwater noise does not interfere directly with the human biological system, although it might affect some of their activities, especially if they are nearby coastal zones (e.g., limitations in military naval systems). Furthermore, it has the potential to mask biological signal communication, and cause direct impact on marine life forms (e.g. porpoises, whales, mammals' echolocation, etc.).

### 2.1.1. Sound Propagation

Sound propagation refers to the way acoustic energy spreads around a source. The sound emitted by a source propagates uniformly (spherically) in an undisturbed or free field but when there are obstacles or variations in the propagation medium properties, sound field is disturbed and it changes the propagation behavior. In general, it can be affected by four important phenomena:

- **Reflection:** Is the change in direction of propagation of a wave due to the interaction with obstacles. In oceans, this phenomenon is commonly happening when sound waves are reflected by the seabed (solid) or the water surface (gaseous).
- **Refraction:** Seawater is not a homogenous propagation medium, it changes its density according to water depth, temperature and chemical properties. Taking into account the last statement, acoustic waves can change direction due to variations in density and temperature, therefore changing the original propagation direction. Figure 1 illustrates the refracted path of a sound wave in water with increasing depth or increasing temperature.

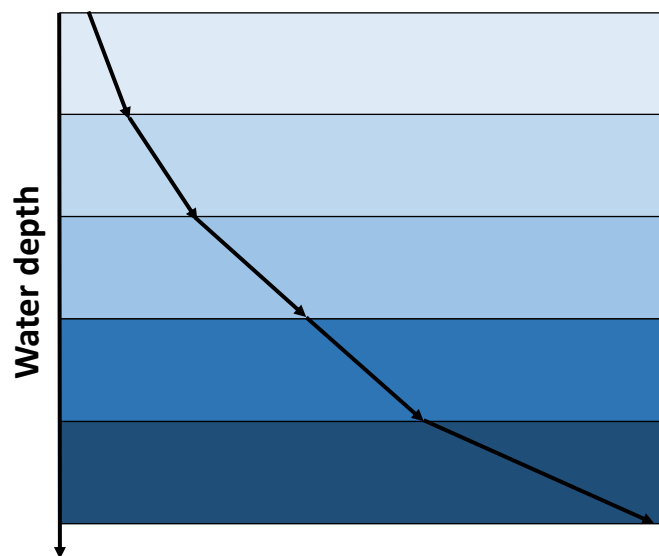


Figure 1. Representation of the refraction of a sound wave in seawater



- **Absorption:** During the propagation of an acoustic wave, part of the energy is dissipated into the propagation medium, which decreases the total energy emitted by the source while the wave is traveling. Usually, the dissipated energy is transformed into heat and absorbed by the medium of propagation.
- **Reverberation:** This phenomenon is caused when changes in direction of the acoustic wave by reflection or refraction create interaction between the waves from one source or between several acoustic signatures. This interaction creates secondary acoustic waves that disturb the ones from the main sources. Besides, some of these secondary waves might be present even when the main source stop emitting.

#### 2.1.1.1. Acoustic Pressure

The acoustic pressure emitted by the source behaves analogically to the expansion of a balloon, the farther the acoustic waves are from the source, the lower the acoustic pressure magnitude, in a similar way, the thickness of the walls of a balloon decreases while it gets bigger. Therefore, the energy in an acoustic wave is only a fraction of the total emitted originally by a source.

#### 2.1.1.2. Propagation Speed

Sound travels at different speeds depending on the propagation medium properties, the closer the molecules in the medium are one to another, the faster the sound travels. As a result, the propagation speed is the rate at which vibrations in the medium caused by sound pressure travel. Seawater is not a perfect homogenous medium, depending on the local temperature, salinity, and depth, water varies its properties, therefore, propagation speed changes. In the literature, there are several mathematic definitions of the speed of sound in water. (e.g. (Kell, 1970), (Mackenzie, 1981), (Coppens, 1981)). Considering the water properties, and the required measurements accuracy, some equations are more suitable than others, although, it is worth mentioning that as a rule of thumb, in seawater a common practice is to assume it to be 1500 m/s.

## 2.2. Underwater Noise Measurement

Acoustic measurements is an important task in many applications involving oceanography, subsea exploration, underwater communications, and more recently marine life risk detection. Each application has one or several ways to measure underwater sounds, in other words, the corresponding value of the sound pressure. The presence of objects in water can be detected by its acoustic signature, which results in changes in pressure on the propagation medium. A receiver or a hydrophone are devices able to record the acoustic pressure at their respective position and bring as output voltages proportional to the actual pressure.

The main characteristics to consider when selecting hydrophones are:

- **Sensitivity:** Related to the amplitude of the sound being recorded, to avoid nonlinearities and poor signal-to-noise ratio for low amplitude signals.
- **Frequency response:** A frequency that should be high enough to record all frequencies components of interest.
- **Directivity:** Estimation of the response of the hydrophone concerning the direction of the received signal.
- **Dynamic range:** Referred to the amplitude over which the system can measure the sound pressure.

In practice, it is possible to find applications for only one hydrophone, but the scope is quite limited, making more difficult certain analysis; nevertheless, these limitations are relatively simple to overcome when two or more hydrophones are combined, forming what is called as a hydrophone array. Arrays are useful measurement systems that make possible to control the direction properties on the transmission and reception signals, as well as improve signals quality. According to (Monzingo & Miller, 1980), arrays have two important advantages over a simple hydrophone:

- a) They allow having a higher gain, proportional to the number of elements in the array.
- b) Arrays bring more possibilities for measurements because of the relative information between each of the hydrophones (time delay, amplitude difference).

Even though arrays have advantages over other measuring systems, array geometries have to be carefully selected depending on different constraints such as their position, physical and

signal interferences, or underwater cables to name a few (Baron, et al., 2021). The simplest array configuration is that where all elements are the same and equally space distributed in a line. (Sullivan, 2015), mentioned other forms of arrays as the 2-D called planar arrays characterized by rectangles or circles geometries and 3-D with cylindrical and spherical shapes. It is important to mention that depending on the approach of the analysis and performance, it should be selected one or another kind of array.

### **2.2.1. Measurement Parameters**

The process of measuring sound requires more than only suitable instrumentation. Understanding the basic terminology that governs acoustic waves is expected and defining the parameters that assure the minimum requirements for a good data measurement practice, as are defined below.

#### **2.2.1.1. Wave Pressure Amplitude**

The amplitude of an acoustic wave represents the pressure recorded by the receiver, which is directly related to the acoustic energy in the wave. Depending on the application, sound pressure has different mathematical definitions, including but not limited to:

- Zero to peak sound pressure ( $A_{PK}$ ).
- Peak to peak sound pressure ( $A_{PP}$ ).
- Root mean square sound pressure ( $A_{RMS}$ ).

#### **2.2.1.2. Wave Pressure Frequency**

The wave frequency refers to the number of oscillations per unit of time. It is represented by  $f$  and measured in Hertz or cycles per second. As will be described in the next section, wave signals from water environments are complex enough to be represented by not one but many frequencies.

### 2.2.1.3. Pressure Wave Period

Taking into account the definition of frequency stated previously, the period of a wave is the inverse of the frequency. Instead of the number of oscillations, period represents the time it lasts for a signal to make a whole oscillation. It is represented by  $T$  and expressed in units of time (s, min or h). In Figure 2, it is represented a simple acoustic wave with the parameters already defined.

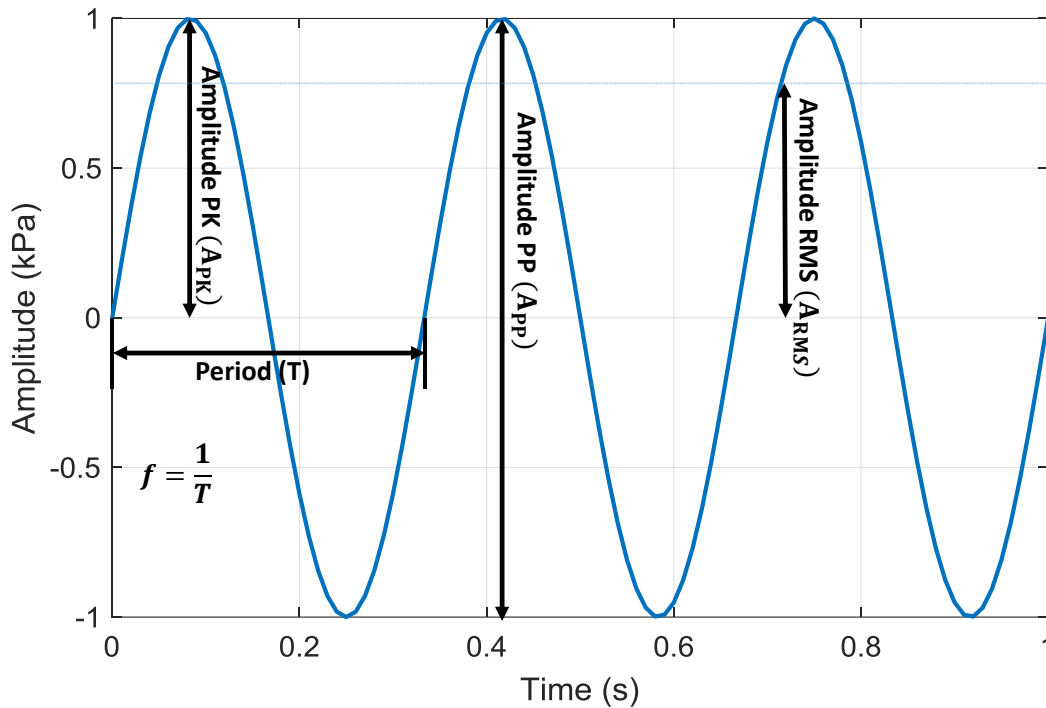


Figure 2. Acoustic signal basic parameters

### 2.2.1.4. Wavelength

This property describes the distance traveled by a wave during one period ( $T$ ). Usually, this value is measured between two consecutive peaks of the wave, but in theory, it can be estimated using two points separated in time by one period. It is represented by  $\lambda$ , and measured in units of distance. Furthermore, it can be related to the wave frequency according to expression 1.

$$\lambda = \frac{c}{f}$$

1

where  $c$  is the propagation speed.

### 2.2.1.5. Phase

Two wave signals with the same frequency (or period) can be related to each other through a phase. This parameter represents the delay or advance of one signal with respect to another. This is represented by  $\phi$  in degrees or radians, but it also can be found in units of time.

### 2.2.1.6. Sample Frequency

This parameter corresponds to the frequency of discrete recording of the acoustic signal. To select it, the user must follow the Nyquist-Shannon sampling theorem (Shannon, 1949), that in a few words, states that the sampling frequency ( $f_s$ ) must be higher than twice the expected frequency to measure ( $f$ ). Thus,

$$f_s > 2f \quad 2$$

### 2.2.1.7. Design Frequency

Every measurement system has its measuring limits, where the quality of measurement is optimized. In this aspect, hydrophones arrays are not the exception, and their design frequency allows the measurements to be focused on a specific range of frequencies. Since, this frequency is dependent on the separation distance between hydrophones, a design frequency is set if the distance between the hydrophones is fixed. On the other hands, if the design frequency is fixed, then the effective distance between the hydrophones can be estimated.

## 2.2.2. Signal Processing

Underwater acoustic signal processing includes all techniques applied to a set of recorded data to give them a physics meaning about the phenomenon intended to identify. The data obtained from the measurements might be useful for real-life applications like detection, classification, localization, or tracking of sources, if and only if the signal processing evaluation is correctly carried out. Some of the signal processing tools used in this project are described in the next sub-sections.

### **2.2.2.1. Band Filter**

Filtering a signal provides a practical way to restrict the frequency content of the signal before using it for the expected analysis. Usually, a signal is filtered to reduce the influence of certain frequencies that are of no interest to the user and might affect the interpretation of the measurements. The most common filters found in signal processing are:

- High pass filter: designed to cut off frequencies less than a specified frequency.
- Low pass filter: to cut off frequencies higher than a specific frequency.
- Band filter: allows component in a specific band of frequencies and block the rest, above or below this band) are of common use in any signal processing application.

### **2.2.2.2. Octave Band**

In acoustic is common to express the sound pressure amplitude in regular ranges of frequency, commonly called frequency bands. The most commonly used are the 1 and 1/3-octave bands that differ in the bandwidth to represent the behavior of the signal. Generally speaking, an octave is defined as a 2:1 ratio of two frequencies, which allows a wide range of possibilities for the band to use, as a result, (ANSI, 2004) set the specification for the estimation of the octave bands that are of most common use in acoustic applications.

### **2.2.2.3. Spectrogram**

Time-frequency analysis might be useful when a representation of the change in frequency in time of a signal is required. For instance, from Figure 3a and Figure 3b, the two signals provide the same frequency spectrum, but just with that information is hard to recreate the behavior of the original signals. A spectrogram is a time-frequency representation of a signal using the short-time Fourier transform as the basis. Figure 3.c and Figure 3.d represent the spectrograms of the signals.

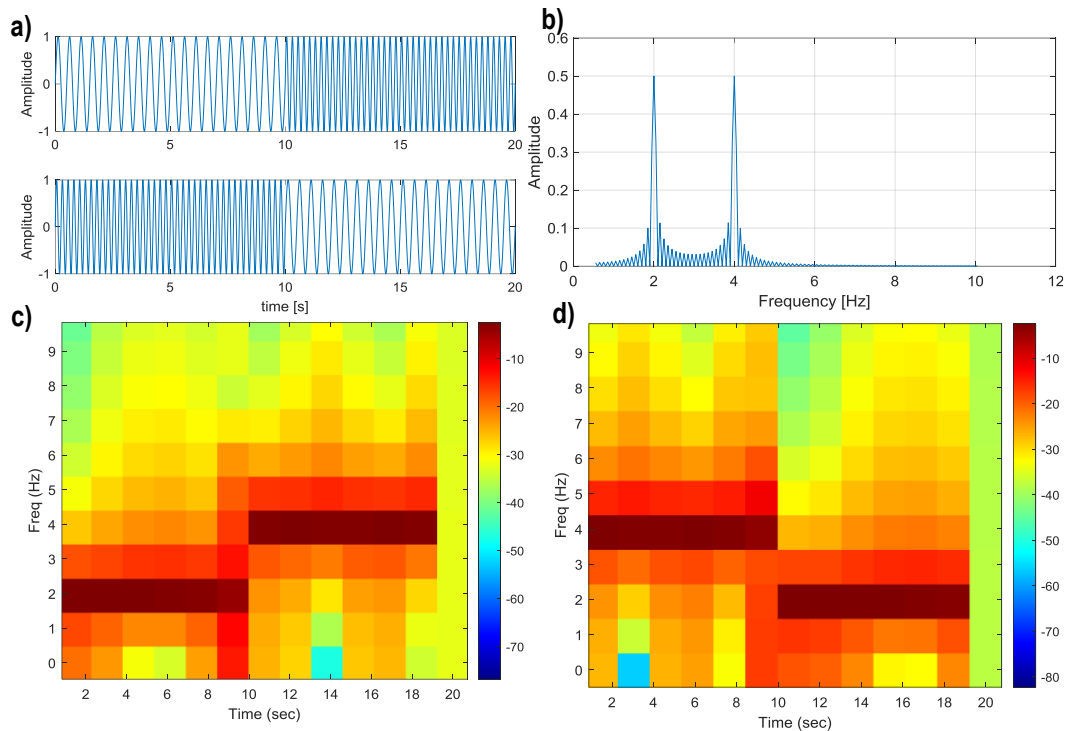


Figure 3. a) Two sinusoidal signals with frequency variation in time. b) Frequency spectrum of both signals. c) Spectrogram of signal 1 (up) d) Spectrogram of signal 2 (down)

The basic idea of the spectrogram is to divide the signal into shorter signals, and then compute a frequency domain analysis (e.g., Fast Fourier Transform) to each segment. The signal windows must be carefully defined depending on the signal features, for example, short windows offer good time resolutions but bad frequency resolutions. In the same order of ideas, long windows offer good frequency resolution but decrease the time resolution. The general scope is finding a balance between both to get a readable representation.

### 2.2.3. Sound Pressure Level

Because of the wide range of sound pressure used in practice (Pohlmann & Everest, 2009), pressure units are inconvenient to use in graphs and tables. A more suitable unit is the Bel (B), a logarithmic unit that relates a value of interest to a reference value that depends on the propagation medium. One decibel (dB), referred as one-tenth of a Bel, is the common unit to measure the intensity of a sound as well as compare sounds. For instance, a sound 100 times more powerful than another represents a difference of 20 dB. Equation 3 shows the expression of a level regarding the sound intensity.

$$L = 10\log_{10} \left( \frac{I}{I_0} \right) [dB] \quad 3$$

where  $I$  and  $I_0$  are the sound intensity and the reference value depending on the propagation medium.

Regarding the sound pressure level (SPL), the proper definition is the ratio of the mean square sound pressure over a stated time interval to the reference value of sound pressure, mathematically expressed as:

$$SPL = 10\log_{10} \left( \frac{p^2}{p_o^2} \right) = 20\log_{10} \left( \frac{p}{p_o} \right) [dB] \quad 4$$

where  $p_o$  is  $2 \cdot 10^{-5}$  Pa and  $1 \cdot 10^{-6}$  Pa, for air and water, respectively.

As can be noticed in equation 4, it must be taken into account carefully the reference value to get a correct estimation of signal level.

### 2.2.3.1. Signal to Noise Ratio

The definition of background noise considers all but the radiated noise from the concerned source, which is defined as a signal in the Signal to Noise Ratio (SNR) expression. Sources generating background noise can be of many origins: sea surface (wind and wave action), biological (marine ecosystem), geoacoustics (natural seismic movement), and traffic (ships and research equipment).

SNR is a comparison between the noise levels of the source of interest (signal) and the background noise (noise), to evaluate the signal quality and quantify the degree of signal-masked problems. The higher the SNR the better the signal quality. One common definition of SNR is shown in equation 5.

$$SNR = 10\log_{10} \left( \frac{S_{RMS}^2}{N_{RMS}^2} \right) = 20\log_{10} \left( \frac{S_{RMS}}{N_{RMS}} \right) [dB] \quad 5$$

where  $S$  and  $N$  refer to the acoustic pressure of the signal and the background noise, respectively.



### 2.3. Underwater Radiated Noise of Recreational Craft

Nowadays, big ships' presence can be easily (and accurately) detected by either radar or AIS systems. The noise radiated by this kind of ship has been widely studied for many years (Arveson & Vendittis, 2000), (McKenna, et al., 2012), (Hallander & Johansson, 2015), etc., and it is characterized by low frequencies (Tesei, et al., 2010). On the other hand, smaller ships like recreational boats are more difficult to detect because of their relatively weak acoustic signature.

Recreational power boating is a relatively new activity, commonly seen in the coastal region but even today, information about the noise they radiate to water is limited and not widespread. (McCarthy, 2004), refers that not only a little amount acoustic data exists for this kind of ship, but also their frequency ranges are generally higher than in big vessels such as carriers or tankers and is highly dependent on their operating status.

The acoustic signatures of small and mid-sized craft have fundamental frequencies from hundreds to 5-6 kHz (Tesei, et al., 2010), which are much higher than the ones found for big ships (most energy below 1 kHz). Moreover, the number of recreational ships has increased over the years as is observed in Figure 4, and considering the high degree of uncertainty about the noise pollution produced by them, several marine species (fish, crustaceans, mammals, and turtles) could be affected at important levels.

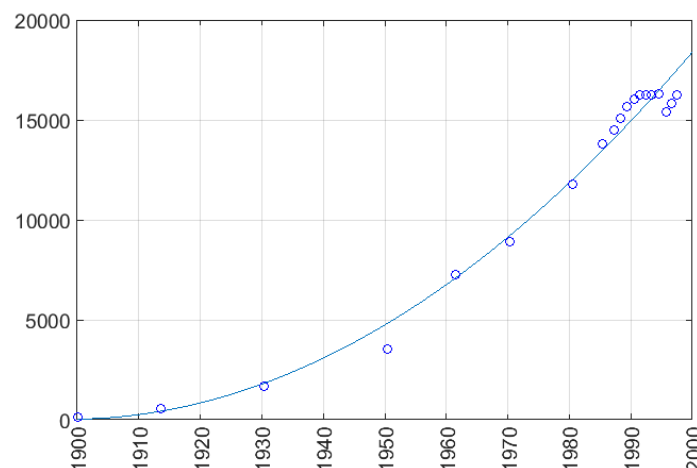


Figure 4. Estimated number of recreational boats owned. (McCarthy, 2004)

The signal of interest regarding these craft come from propeller cavitation (Wittekind, 2017) and the hull interacting with the sea surface, as well as their close-packed high-powered propulsion equipment, confined in small structures.

## 2.4. Sound Detection

This is a binary problem regarding if a source is in a detection range or not. The idea behind a detection algorithm is to identify acoustic signals that surpass an amplitude (or frequency) threshold predefined by the user. To define a suitable threshold it must be considered carefully the ambient noise present during the measurements to avoid sound masking problems that might lead to false outputs from the detection.

## 2.5. Sound Bearing and Localization Methods

The existence of a source in water provided by a detection algorithm brings the next question to the user: Where is it? The position or at least bearing of a source might be estimated with any active or passive methods once its respective acoustic emission is available. According to (Buehrer & Zekavat, 2012), the most fundamental techniques of determining bearing are:

- Received Signal Strength (RSS)
- Time of Arrival (TOA)
- Time Difference of Arrival (TDOA)
- Direction of Arrival (DOA)

In the next subsections, is presented a brief description of the methods, advantages, disadvantages as well as the basic formulations.

### 2.5.1. Received Signal Strength

Received Signal Strength (RSS) methods focus their attention on the wave energy ratio from pairs of receptors to estimate a source position. In terms of measurement complexity, usually, these methods are less complex and easier implementation than time-based methods. However, their performance is highly dependent on the underwater environment conditions, and in most cases requires single dominant sources, which makes them difficult to manage the detection of multiple targets.

The basic formulation of RSS methods is described as follows, based on (Gloza, 2009), (Pourmohammad & Mohammad, 2013) and (Kumar Mahapatra, 2017) works.

Considering two signals with sound power  $P_1$  and  $P_2$ , from two different receptors, assuming unbounded and homogenous propagation medium, sound waves propagate spherically (Wittekind, 2017). According to inverse square law, they can be expressed as:

$$P_1 \propto \frac{1}{d_1^2} \qquad P_2 \propto \frac{1}{d_2^2} \qquad 6$$

where  $d_1$  and  $d_2$  are the distances from the source to each respective receptor, defined as follow:

$$\begin{cases} d_1^2 = (x_1 - x_s)^2 + (y_1 - y_s)^2 \\ d_2^2 = (x_2 - x_s)^2 + (y_2 - y_s)^2 \end{cases} \qquad 7$$

where  $x_s$  and  $y_s$  are the source position coordinates in the plane. In addition,  $x_1, y_1$  and  $x_2, y_2$  are the position coordinates of the receiver 1 and 2. Thus, the two signals energy can be related as:

$$P_1 d_1^2 = P_2 d_2^2 \qquad 8$$

Equations 7 and 8 form the system 9:

$$\begin{cases} P_2 d_1^2 = P_1 d_2^2 \\ d_1^2 = (x_1 - x_s)^2 + (y_1 - y_s)^2 \\ d_2^2 = (x_2 - x_s)^2 + (y_2 - y_s)^2 \end{cases} \qquad 9$$

Notice this represent the equations of two circles that coincide in two points, creating an ambiguity in the solution. To solve the system, it is possible to add another receiver to find the interception coordinates of the three circles.

### 2.5.2. Time of Arrival

Time of arrival (TOA) method focus on the time of propagation of the waveform from the source to each receptor. On the contrary to the RSS methods, in this case, the amplitude of the signal is not relevant for the position estimation. TOA uses information regarding the time the wave starts traveling and the time is received by each receptor. The formulation of the method is described as follows:

If  $t_1$  is the time that takes to receptor 1 to detect the source signal, the distance source-receptor  $d_1$ , can be expressed as shown in equation 10.

$$d_1 = ct_1 = \sqrt{(x_1 - x_s)^2 + (y_1 - y_s)^2} \quad 10$$

where  $c$  is the propagation speed.

The system requires at least three equations, thus, three hydrophones are needed, and two similar equations can be expressed as:

$$d_2 = ct_2 = \sqrt{(x_2 - x_s)^2 + (y_2 - y_s)^2} \quad 11$$

$$d_3 = ct_3 = \sqrt{(x_3 - x_s)^2 + (y_3 - y_s)^2} \quad 12$$

Then, the system of equations to solve is:

$$\begin{cases} d_1 = \sqrt{(x_1 - x_s)^2 + (y_1 - y_s)^2} \\ d_2 = \sqrt{(x_2 - x_s)^2 + (y_2 - y_s)^2} \\ d_3 = \sqrt{(x_3 - x_s)^2 + (y_3 - y_s)^2} \end{cases} \quad 13$$

As can be observed from system 13, the equation represents the three circles, where the common point represents the estimated position of the source (Figure 5).

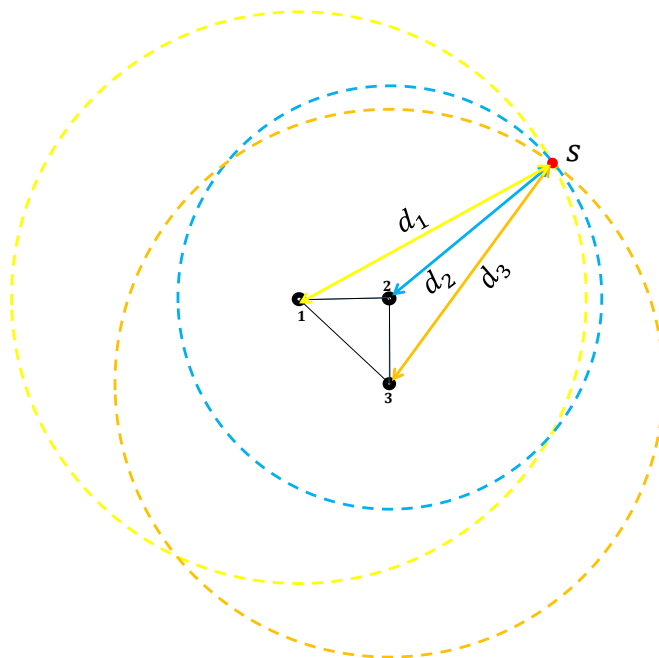


Figure 5. TOA approach with three receivers to locate a source

It is worth noticing that if are considered less than three receivers, a unique solution cannot be obtained (Same for RSS approach).

### 2.5.3. DOA & TDOA Principles

Direction of Arrival (DOA) and Time Delay of Arrival (TDOA) are highly related in their formulations for bearing and positioning estimation. In this section, a brief description of the method is carried out.

#### 2.5.3.1. 2-Hydrophones Array

The main advantage of DOA over TDOA method is that the first one can be applied with only two receptors available, not the case for TDOA, which requires at least three as is described in the next section.

To estimate the direction of arrival, consider a source at a certain distance from the linear array. As can be seen in Figure 6, if the source is far enough from the array, when its waves reach the receptors, the acoustic wave behaves as a planar wave. The difference between the times each receptor detect the source wave, defined as the time delay, can be related to the distance between the receptors, to estimate the angle of arrival. According to the last statement, equation 14 express the angle of arrival.

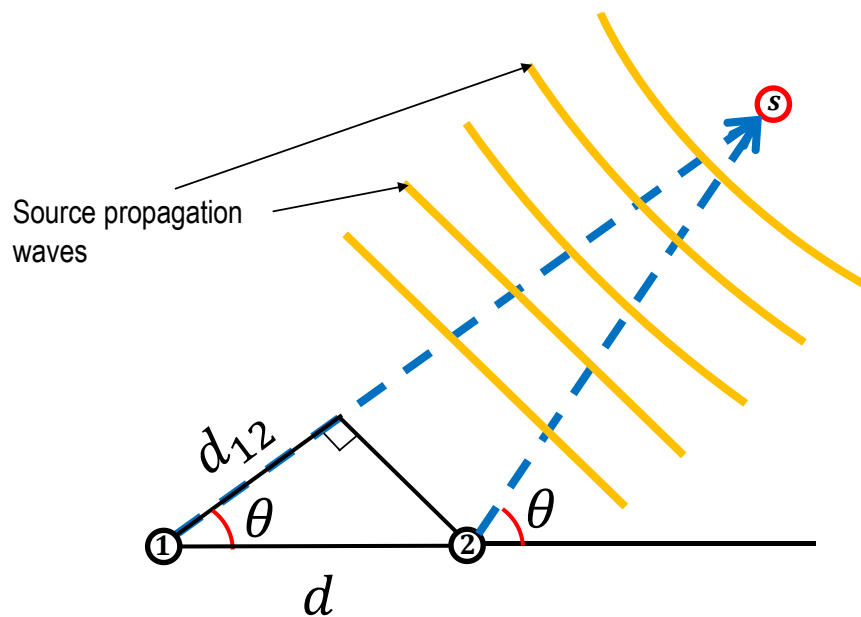


Figure 6. 2-hydrophones linear array

$$\theta = \cos\left(\frac{d_{12}}{d}\right)$$

14

where

$\theta$  is the angle of arrival.

$d_{12}$  is the distance traveled by the wave from one receptor to another one.

$d$  is the distance between the receptors.

Notice that  $\theta$  values are limited to  $0 \leq \theta \leq \pi$ , in other words, with this solution is not possible to assure whether the source is on the right or the left of the array line. This ambiguity problem is a characteristic of linear arrays and depending on the application should be avoided or might be overcome with some extra information from the source. One alternative to avoid the ambiguity is adding an extra hydrophone to the array, one not collinear with the other two, as is described below.

### 2.5.3.2. 3-Hydrophones Array

A 3-receptors triangular array is the minimum requirement to avoid DOA ambiguities in a 2-receptors array. Figure 7, shows each pair of receptors, and how they bring two possible angle solutions, where one is the true direction of arrival and the other is a phantom or a false direction. As a result, combining the four results, only two of them will match, allowing estimating the right bearing of the source.

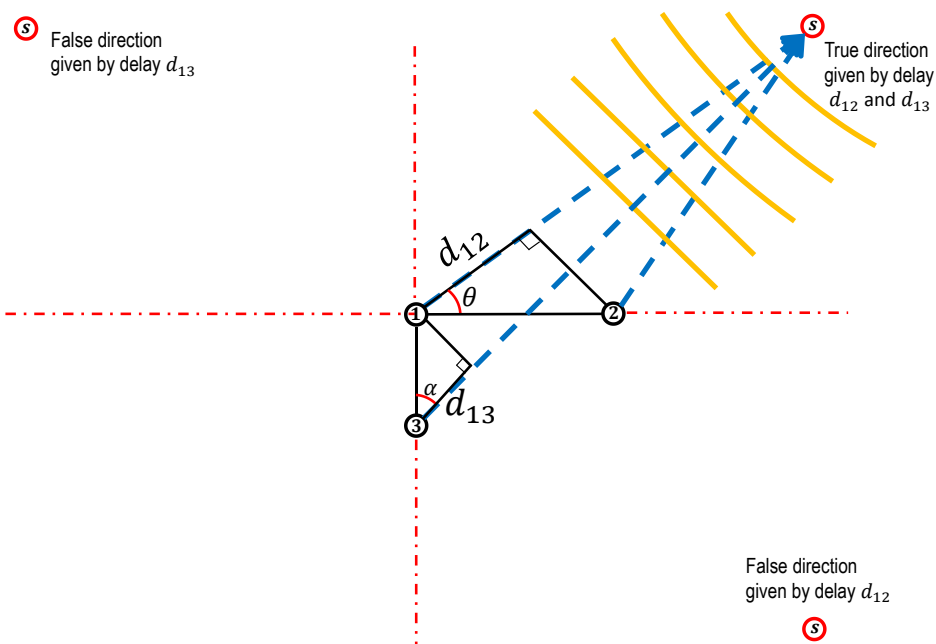


Figure 7. 3-hydrophones planar array (DOA)

In addition, from Figure 7 it can be developed TDOA formulation, which requires a minimum of three recorders. The basic idea of the method is described as follows:

Let define  $\mathbf{s}$ , a vector from a coordinate reference system to the source, and  $\mathbf{m}_i$  a vector from the reference to the receptor  $i$ . Then, a vector  $\mathbf{r}_i$  can be defined according to expression 15:

$$\mathbf{r}_i = \mathbf{s} - \mathbf{m}_i \quad 15$$

Moreover, considering a pair of hydrophones, equation 16 is satisfied:

$$|\mathbf{r}_i| - |\mathbf{r}_j| = c\tau_{ij} = d_{ij} \quad 16$$

where  $i$  and  $j$  represent the indexes for the first and second receptor,  $\tau_{ij}$  the time delay between the signals of each receptor, and  $d_{ij}$  is the distance traveled by the acoustic wave from one receptor to another one. If all terms from equation 16 are expanded:

$$\sqrt{(s_x - x_i)^2 + (s_y - y_i)^2} - \sqrt{(s_x - x_j)^2 + (s_y - y_j)^2} = d_{ij} \quad 17$$

Notice that a similar equation can be formulated considering another pair of receptor, which creates a system of the equations of two equations and two variables ( $s_x$  and  $s_y$ ). However, is a nonlinear system with multiple solutions.

$$\begin{cases} \sqrt{(s_x - x_1)^2 + (s_y - y_1)^2} - \sqrt{(s_x - x_2)^2 + (s_y - y_2)^2} = d_{12} \\ \sqrt{(s_x - x_1)^2 + (s_y - y_1)^2} - \sqrt{(s_x - x_3)^2 + (s_y - y_3)^2} = d_{13} \end{cases} \quad 18$$

From Figure 8, it can be observed graphically the TDOA formulation.

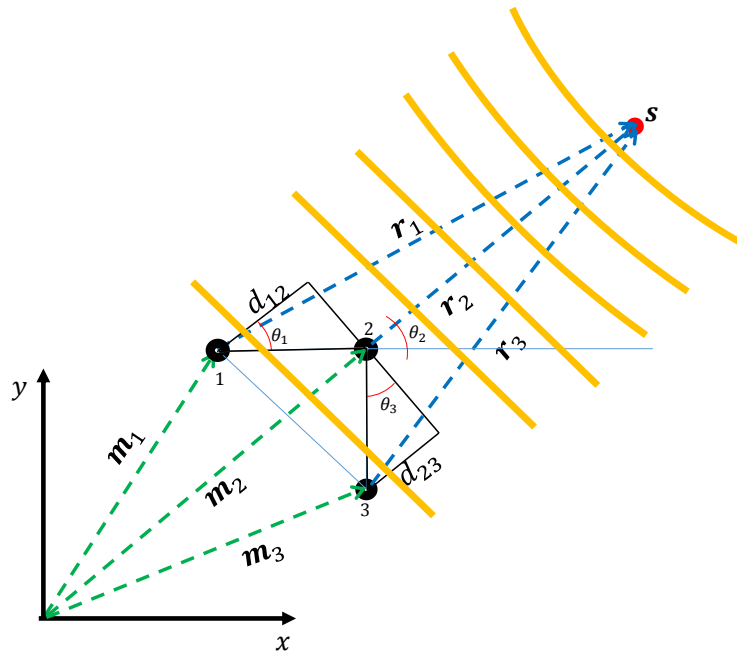


Figure 8. 3-hydrophones planar array (TDOA)

From Figure 8, is possible to estimate three angles, by adding an equation relating receptors 2 and 3, although this is a redundant equation from the others two.

From the methods considered and briefly described in this section, three are localization methods that require solving nonlinear multi-root system of equations, and one of them is bearing estimation which requires solving simpler equations but requires comparing solutions to determine the correct value.

TDOA methods are suitable for one source positioning due to the existence of only one delay per pair of microphones, although, when the same array detects more than one delay, it is not straightforward to decide which delays from pair of receiver 1 match the delays from pair of receiver 2, and so on.

Moreover, to solve the nonlinear problem, (Chapra, 2007), (Ralston & Rabinowitz, 1978), (Militello & Buenafuente, 2007), proposed numerical alternatives to improve the numerical difficulties of TDOA and others like (Buehrer & Zekavat, 2012) suggest adding one extra recorder than the minimum to reduce the nonlinear system to a linear. Nevertheless, difficulties with respect to the delays matching are still present.

Direction of arrival technique has a practical advantage over the other methods; concerning the possibility to detect more than one source more easily. The more relevant weakness of TOA regarding the scope of this work is the need for time synchronization between receptors and



sources, which might be possible when analyzing a research vessel, but not practical for several unknown sources. Similarly, RSS is considered one of simplest methods but the requirement of a dominant source make the approach not practical for multiple targets. Finally, DOA is a relatively easy method to apply and allow the possibility to estimate the bearing of multiple targets.

Table 1 describes summaries the advantages and disadvantages of each of the described methods.

Table 1. Comparison of passive sound localization methods

Method	Advantage	Disadvantage
TOA	Range estimation.	It needs time synchronization. Assumes there is not an obstacle in recorder-source route.
DOA	Time synchronization is not required. Suitable for multiple sources.	Only bearing calculation. Time delay estimation is not straightforward.
TDOA	Range estimation. Time synchronization is not required.	Global solution is not guaranteed. Multiple source estimation is not suitable.
RSS	No time consideration. Simple instrumentation.	Presence of one dominant source is needed. Low accuracy.

Additionally, it worth to consider the localization methods from the mathematic point of view there are limitations to estimate accurately distances much longer than the dimensions of the array (Abraham, 2019). However, to determine the bearing estimation, where only time differences are include in the calculations, bearing estimation of a source would be the primary alternative. (Xunxue, et al., 2018)

Taking into account the previous description, it was considered the Direction of Arrival method for the bearing estimation of the concern sources in this project.

## 2.6. Cross-Correlation Function

The main characteristic of and DOA (and TDOA) method is the use of the time delays between the signal of the receptors. Therefore, the accuracy to estimate the bearing is directly dependent on the accuracy of the measured delays. The magnitude of these delays are influenced by the location of the source and the location of each hydrophone in the array, the closer the hydrophones are to each other, the smaller the delays.

Delays or phase between signals is not a complex. Figure 9, shows the delay between two sinusoidal signals that can be easily calculated by representing the equation of each curve or simply by graphical estimation.

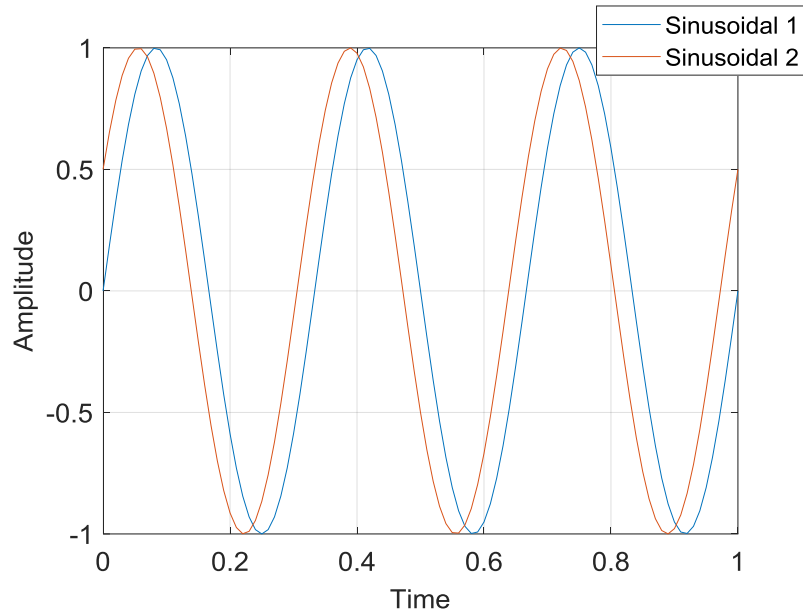


Figure 9. Sinusoidal signals delayed each other

However, in practice, acoustic signals are much more complex and almost identical at a glance, making it difficult the task to estimate the phase difference between them. Figure 10 illustrates the last statement.

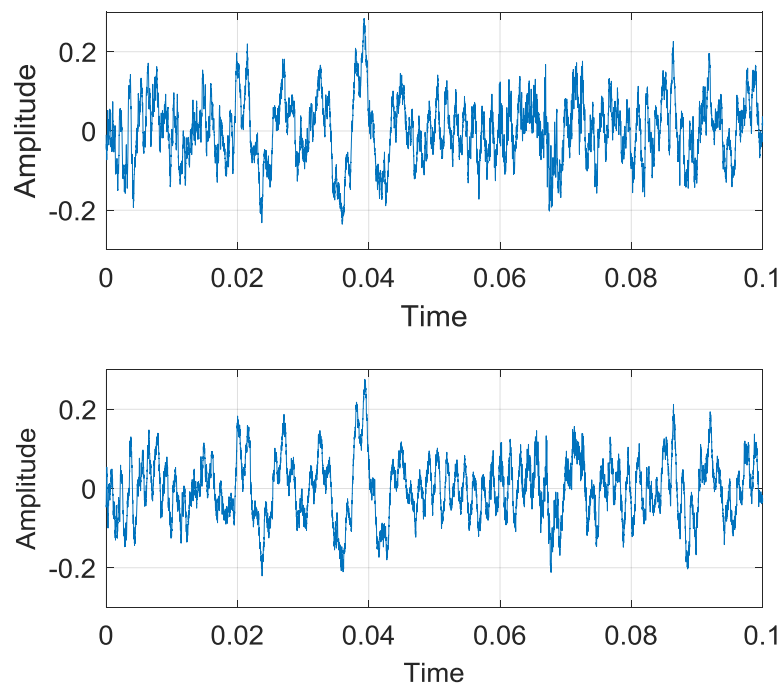


Figure 10. Signals from two hydrophones in a linear array

To overcome the difficulties in obtaining time delays between signals, cross-correlation functions are commonly used. In equation 19 is expressed the cross-correlation function definition

$$R(\tau) = \int_{-\infty}^{\infty} x(t)y(t + \tau)dt \quad 19$$

where  $x(t)$  and  $y(t + \tau)$  are the signals to compare

and  $\tau$  is the time delay

It is important to mention that the received signals  $x$  and  $y$  are similar in amplitude and frequency, but with a time shift.

The basic idea of this method is displacing one signal relative to the other, comparing point by point of the two of them. At the same time, the similarities are stored as a cross-correlation function and is possible to plot to observe the sections where similarities are more relevant. Figure 11 illustrates the cross-correlation function steps of two one simple signals.

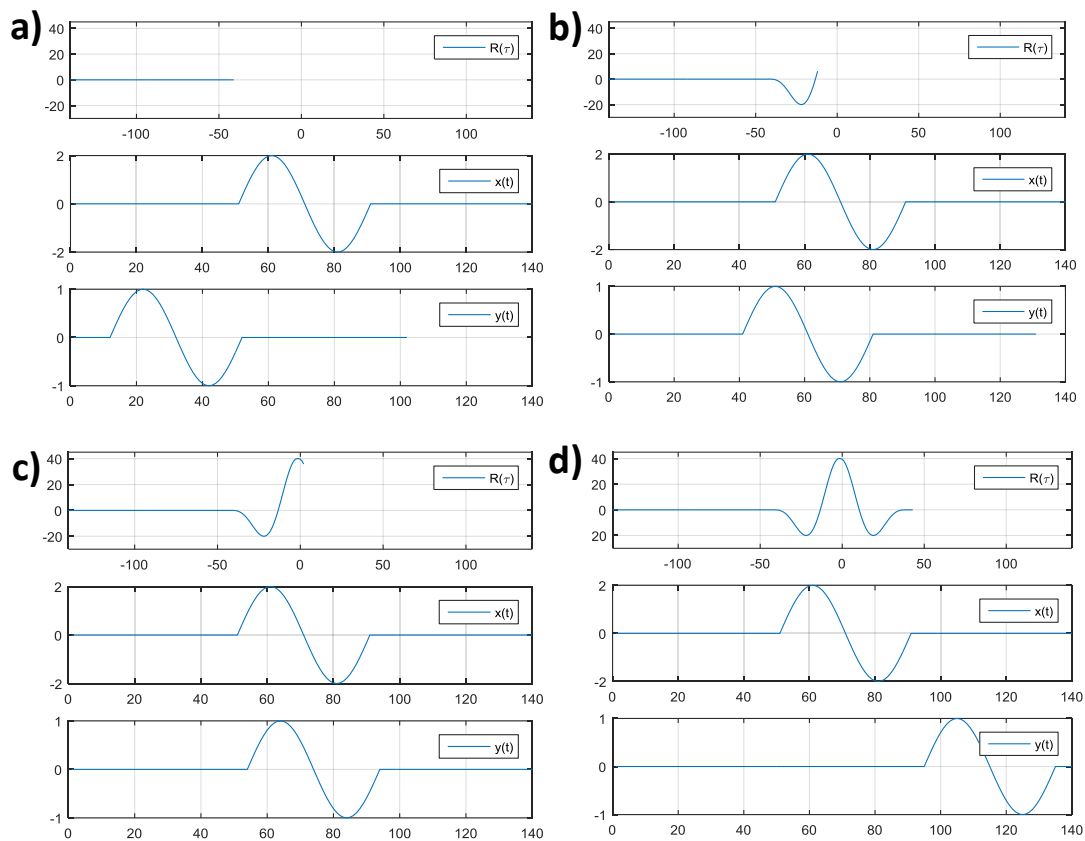


Figure 11. Cross-correlation steps of a simple wave signal

### 3. METHODOLOGY

In this chapter is described the validation of the proposed Direction of Arrival model (DOA) and the design of the measurement system. At first, it was validated the DOA model with a 2-microphones linear array by estimating the bearing of a source and two sources at the same time. Secondly, it is described the design steps of the 4-hydrophones array measurement system. Finally, the system building steps and deployment process are explained.

#### 3.1. Validation DOA Model with a 2-Microphones Linear Array

For the validation of the DOA model formulated in the previous chapter, it was proposed a linear array in air with two microphones. The total measurement system consisted of two microphones (B&K and PCB), an A/D converter, and a signal analysis LabView program (for detailed specifications refer to Table 2).

Table 2. Recording system specification two hydrophones linear array

Part	Make	Sensitivity / Version	Serial No.	Calibration Date
Microphone B&K	B&K 4188-A-021	30.1 mV/Pa	2756790	19.08.2011
Microphone PCB	PCB 130E20	43.4 mV/Pa	SN 42348	
A/D Converter	National Instruments (NI) 9234		1DF0EF2	23.09.2019
Laptop Computer	Lenovo Yoga 370	-	n/a	
Signal Analysis S/W	NI LabView Incl. Sound&Vibration Suite	Version 2015	n/a	

The proposed validation experiment consisted in estimate the direction of arrival of a source in 9 different known positions, varying the angle range (0-180°) and radius of a semi-circle (3-18 m) from the array, detailed in Figure 12. The proposed targets were a 1 kHz sinusoidal signal and the radiated underwater noise from a motor boat taken from (Santos-Domínguez, et al., 2016) database. In addition, it was proposed a final case using the recording of another motor boat from (Santos-Domínguez, et al., 2016) to study the performance of the model with more than one source at the same time.

Figure 12 details the different positions selected to place the sources and the position of the 2-microphones array.

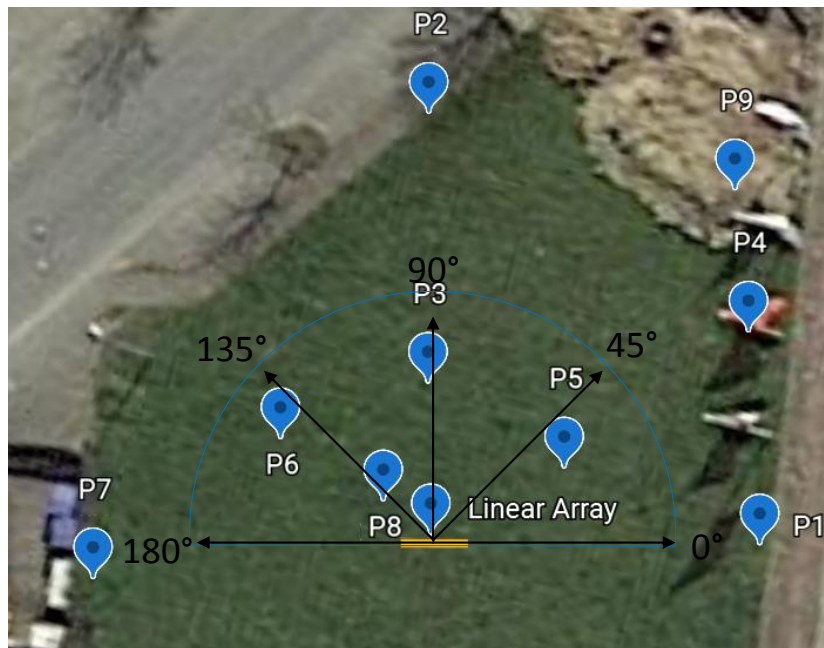


Figure 12. Source positions

Table 3 shows the conditions and specifications of the array (Figure 13)

Table 3. Condition and specification of the linear array

Location coordinates	54°17'28"N 10°13'36"E
Average temperature	10°C
Design Frequency	1 kHz
Distance between microphones	16.5 cm
Speed of sound	337.24 m/s



Figure 13. B&K-PCB Microphone linear array

Taking into account the first testing signal, a 1 kHz frequency sinusoidal, it was set the design frequency by adjusting the distance between the microphones. In this case, the distance was set to 16.5 cm, but depending on the target frequency that distance can be varied to higher frequencies (by reducing microphones separation distance lower than 16.5 cm) or lower (by setting separation distance higher than 16.5 cm).

Once the separation distance between the hydrophones was calculated, it proceeded to assemble the recording system, and identify the spots expected to place the sources (Figure 12). With the recording system in position, the validation experiment was carried out according to the steps described below:

- 1) The speaker meant to radiate sources acoustic signal was placed on measurement point 1 ( $M_1$ ).
- 2) The recording started measuring background noise for 10-30 seconds, and then the speaker played the source-testing signal.
- 3) The speaker sound stopped emitting sound, and the quality of the recorded quality evaluated. In case of an unsuccessful recording, it repeated the previous step.
- 4) The procedure was repeated from step 1), considering the next measurement point.

Figure 14 shows the recorded signals at  $P_4$ , where can be detailed the background noise (lower amplitudes sections) and concern testing signal (higher amplitude section).

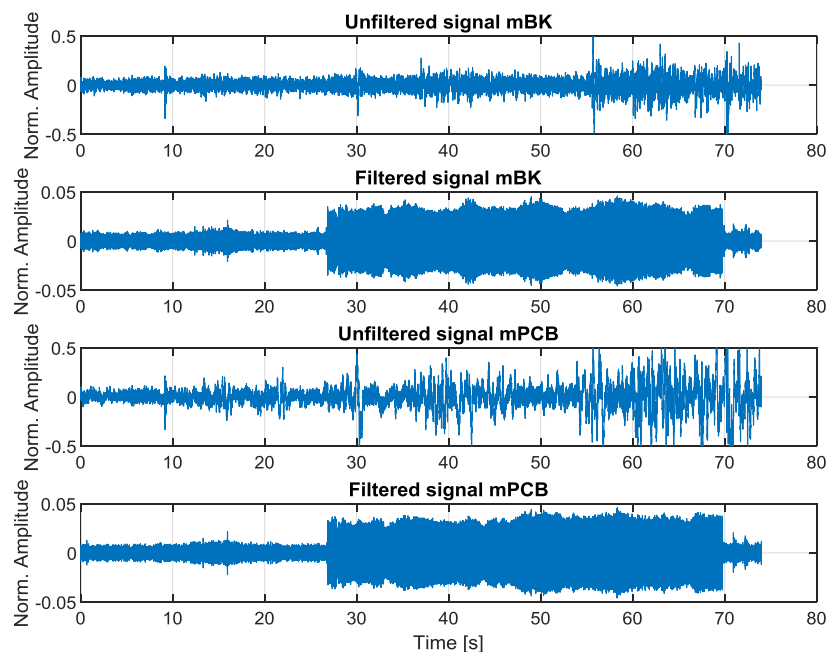


Figure 14. Recording of microphones of 1 kHz signal at  $P_4$

In addition, Figure 15 shows the octave spectrum of the background noise and the 1 kHz sinusoidal signal, respectively. As can be seen, the background noise is more high amplitudes at low-frequency bands but after 63 Hz, the tendency is that background noise is less relevant in the signal, especially at the concerned frequency (1 kHz). Hence, this allowed pre-analyzing the information and verifying whether background noise was masking the target signal before applying DOA routine.

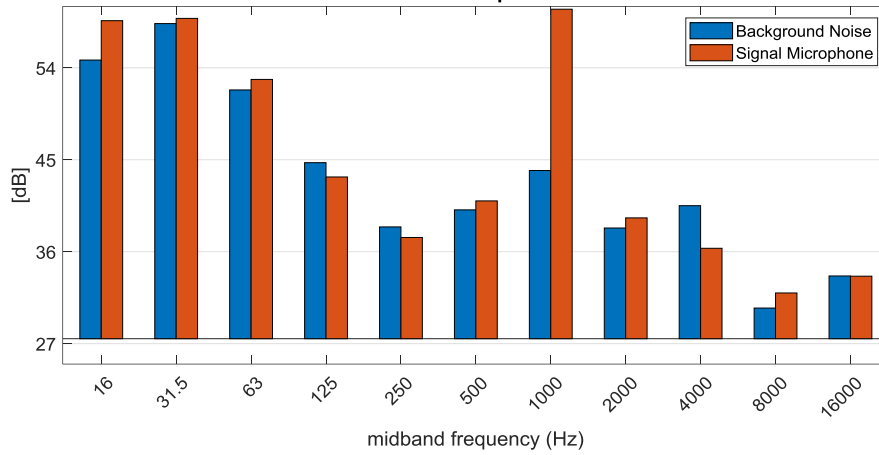


Figure 15. Octave spectrum of 1 kHz at P<sub>4</sub>

In the same order of ideas, Figure 16 represents the signal recorded using the motor boat signal at measurement point 4 (see Figure 12). In this case, the signal shows a similar behavior comparing ambient noise and target signal, noticing differences between the levels (Figure 17), and for the design frequency, background noise apparently is not masking the signal.

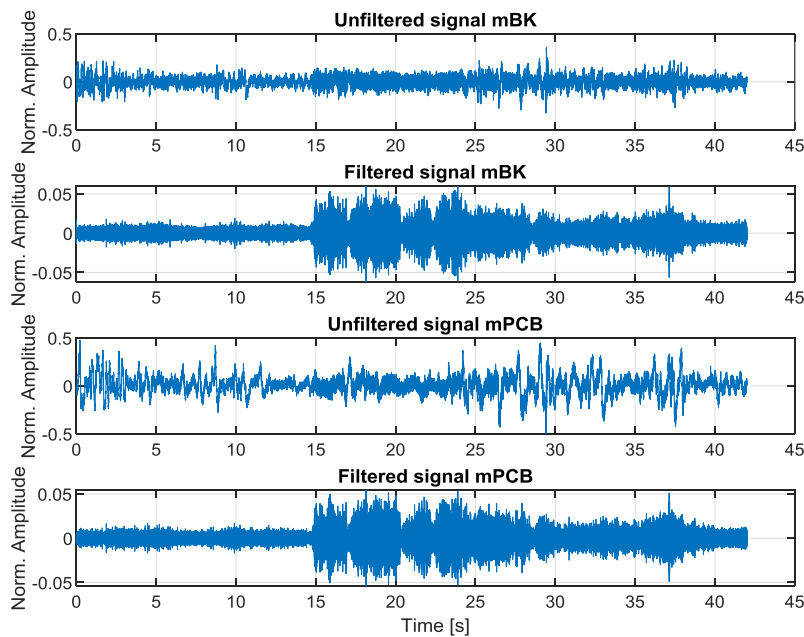
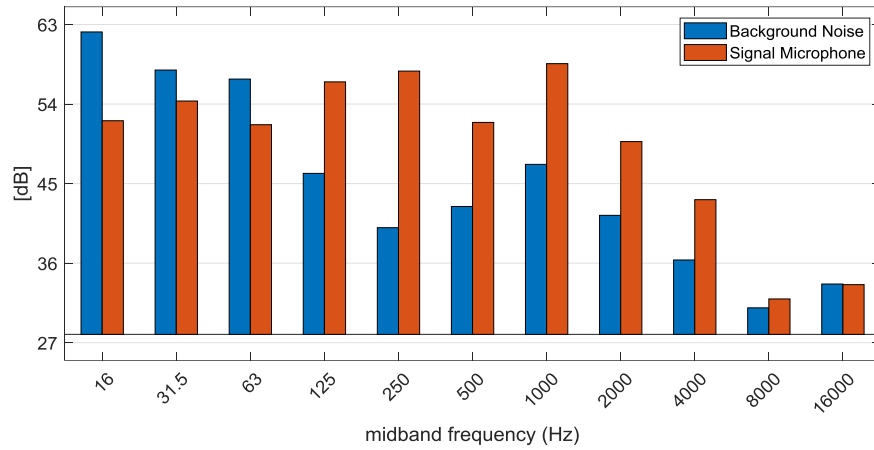


Figure 16. Recording of microphones of motor boat at P<sub>4</sub>

Figure 17. Octave spectrum of motor boat at P<sub>4</sub>

In Figure 18 and Figure 19, can be found the octave spectrums regarding the rest of the measurements for both cases. In addition, the analysis regarding all of them about the quality of the recorded signal is similar to the ones above.

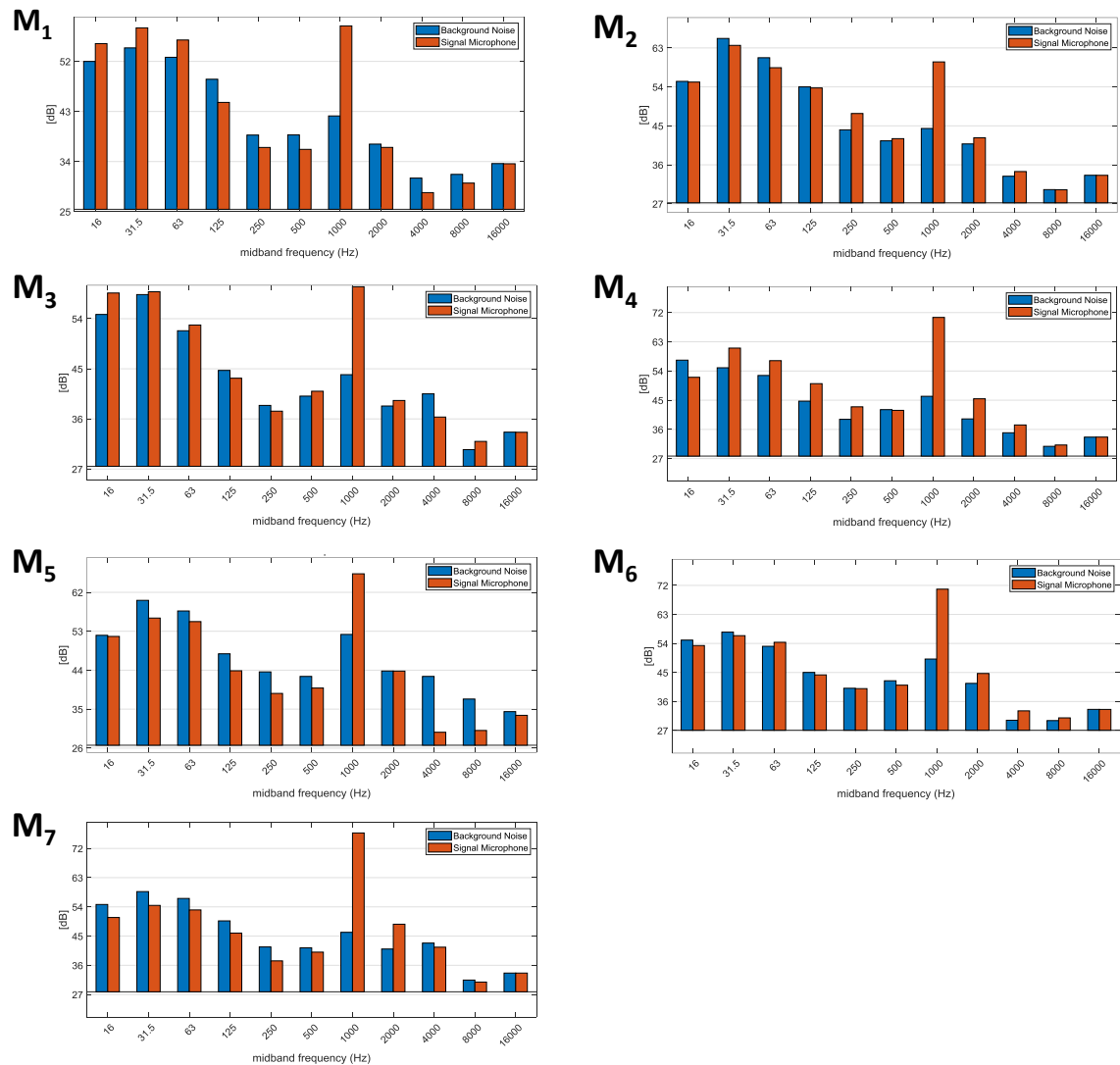


Figure 18. Octave spectrum of 1 kHz sinusoidal



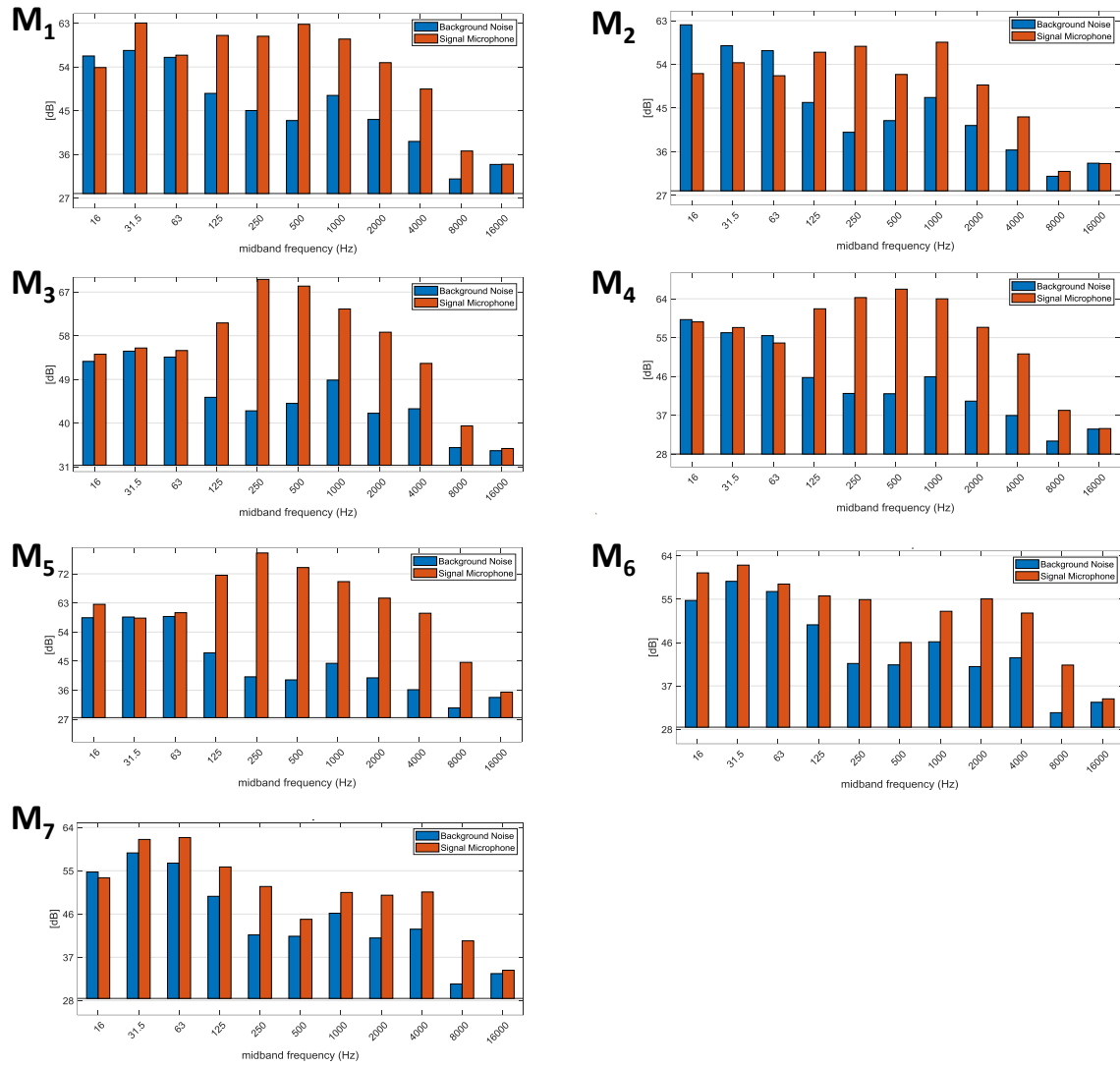


Figure 19. Octave spectrum of motor boat signal

After a detailed screening of the recorded signals, it proceeded to apply the DOA model routine, which includes the time delay estimation using a cross-correlation function.

As was described in the previous chapter, usually the maximum peak of the cross-correlation function is the delay. However, when more than one delay is expected a more detailed analysis should be considered. With respect to the last statement, it was evaluated two cases with two motor boats at different positions ( $P_1$  &  $P_2$  and  $P_2$  &  $P_9$ ). Figure 20 shows the cross-correlation function obtained once it was evaluated the signals at spots  $P_2$  and  $P_9$ . Moreover, Figure 21 represents the peaks of envelope of the cross-correlation plot.

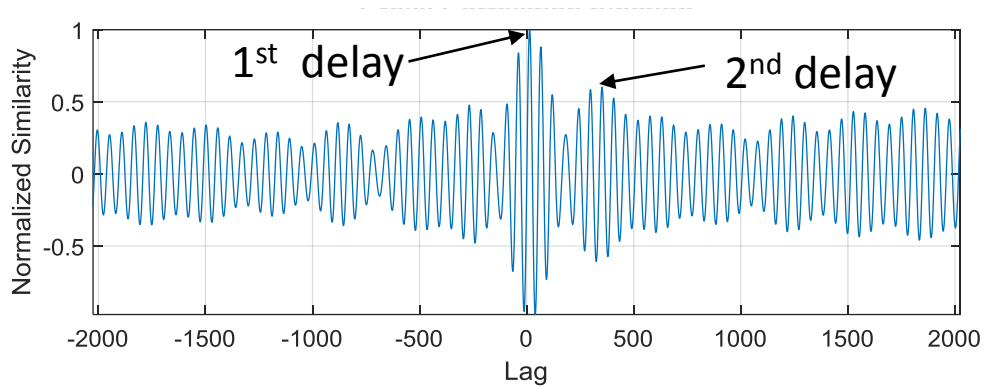


Figure 20. Cross-correlation function

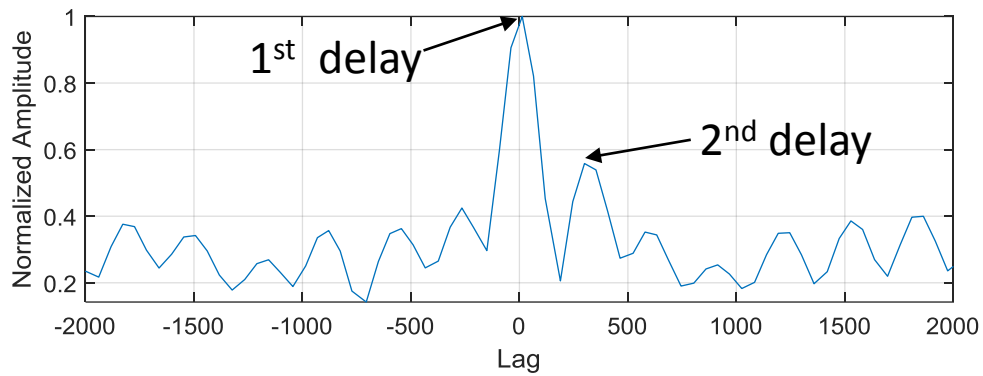


Figure 21. Cross-correlation peaks function

In general, to estimate the correct peaks, it was not enough to use only the cross-correlation function but together with its peak function eases to detail the behavior of similarities between the two signals. Despite the fact, it can be observed several peaks, after setting a threshold of around 60%, based on the lack of relevance from the other peaks; it was successfully detected the presence of both sources.

Once the described methodology was applied to all the measurements, it proceed to estimate the bearing in each case and compare them with the expected angles. Figure 22 shows the bearing considering the 1 kHz sinusoidal signal in seven different locations.

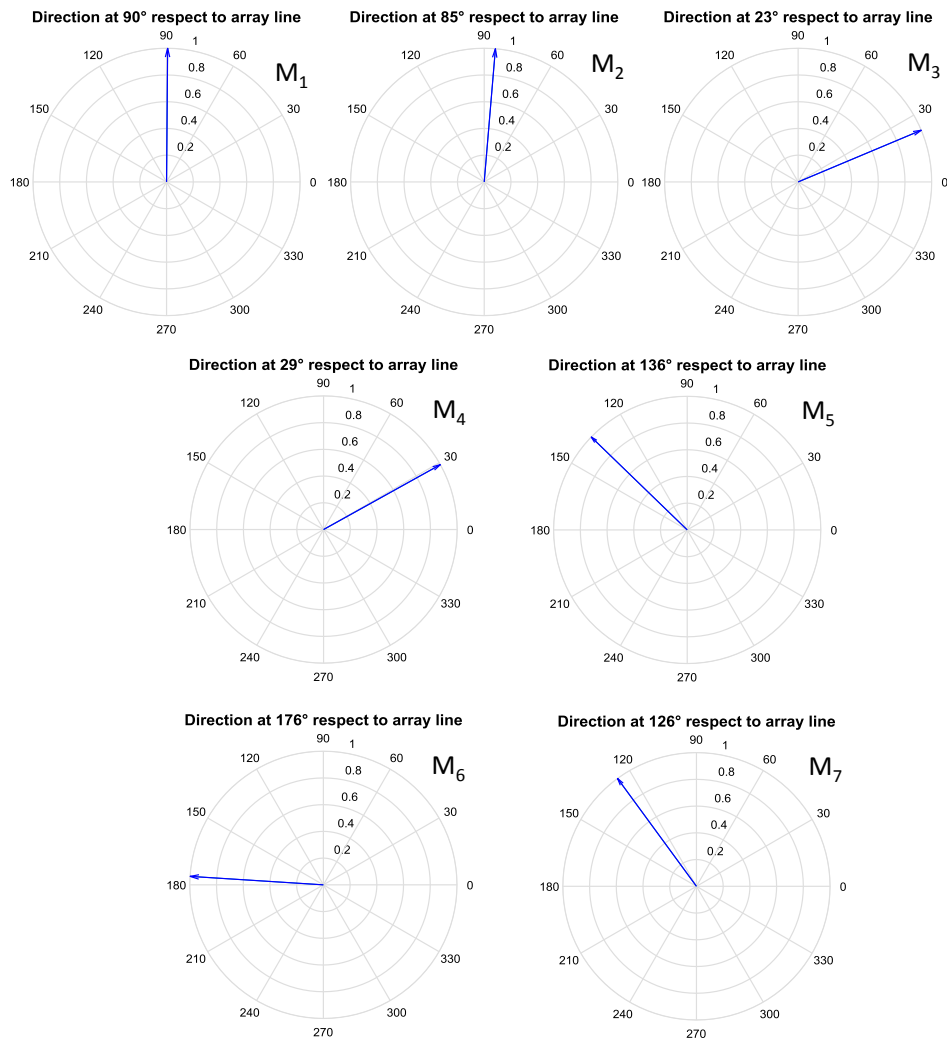


Figure 22. Bearing of sinusoidal wave signal

In addition, Table 4 shows the expected and calculated bearings, as well as the absolute error between them.

Measurement	Source position point	Direction expected [°]	Direction obtained [°]	Difference [°]
M <sub>1</sub>	P <sub>2</sub>	99	90	9
M <sub>2</sub>	P <sub>3</sub>	98	85	13
M <sub>3</sub>	P <sub>4</sub>	29	23	7
M <sub>4</sub>	P <sub>5</sub>	24	29	5
M <sub>5</sub>	P <sub>6</sub>	149	136	13
M <sub>6</sub>	P <sub>7</sub>	186	176	10
M <sub>7</sub>	P <sub>8</sub>	134	126	8

From Figure 22, it is important to notice that all results were limited to the range  $[0-180]^\circ$  because it was used a linear array and the ambiguity problem discussed in the previous chapter was present. However, considering the locations of the source are known with respect to the

array (Figure 12), the solution was restrained to the right zone to avoid a discussion about ambiguities that are well-known to exist in this kind of array. In the same order of ideas, Table 4 shows that the maximum error obtained was  $13^\circ$ , which is remarkable considering the source was placed at a distance between 3-18 m from the array, and the experiment was carried out only with two microphones separated only by 16 cm. Besides, this validation was accomplished in an uncontrolled environment.

Similar to the previous case, Figure 23 and Table 5 detail the obtained results but using the motor boat signal.

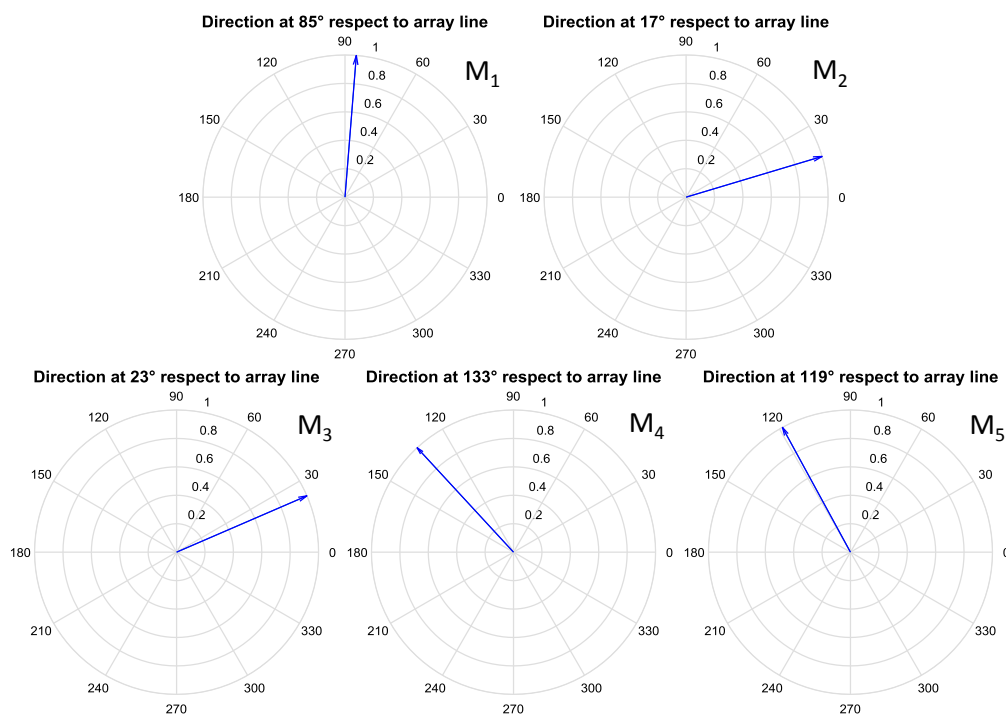


Figure 23. Bearing ship signal

Table 5. Bearing from Motor boat signal

Measurement	Measurement point	Direction expected $[\circ]$	Direction obtained $[\circ]$	Difference $[\circ]$
M <sub>1</sub>	P <sub>3</sub>	98	85	13
M <sub>2</sub>	P <sub>4</sub>	29	17	12
M <sub>3</sub>	P <sub>5</sub>	24	23	16
M <sub>4</sub>	P <sub>6</sub>	149	133	16
M <sub>5</sub>	P <sub>8</sub>	134	119	15
M <sub>6</sub>	P <sub>1</sub> & P <sub>2</sub>	0 and 99	30 and 90	30 and 9
M <sub>7</sub>	P <sub>2</sub> & P <sub>9</sub>	99 and 53	90 and 52	9 and 1

In this case, it used similar measurement positions to the previous case, and results showed similar behavior, despite the fact, that this signal represents a more complex source than a 1

kHz sinusoidal. Expect from the  $30^\circ$  error found on the  $M_6$ , the maximum absolute error was  $16^\circ$ , an important result that shows more about the validation of the DOA method. Besides, notice for the two sources' cases, the errors were even lower than most of the one source cases. Regarding the bearing error estimated on  $P_1$  bearing,  $30^\circ$  far from the correct value, still in the correct quadrant and relatively close to the solution.

Finally, considering the obtained results, bearings of one and two sources, with a simple array in uncontrolled conditions and all the different cases evaluated, it was confirmed the validation of the DOA method.

### 3.2. 4-Hydrophones Planar Array Design Stage

DOA validation for bearing estimation of multiple sources was a necessary step before starting with the 4-hydrophones array design proposed in this work. With this, the core of the routine to estimate bearings was established to be apply it to more complex arrays in more complex environmental conditions. Furthermore, the proposed measurement system was expected to avoid ambiguity problems due to the 4-receivers configuration in a no collinear shape.

The measurement system is based on a 4-channels RTSys EA-SDA14 acoustic recorder and 4 hydrophones with a sensitivity of  $[-172 \pm 2]$  dB re  $1\mu\text{Pa/V}$ . The deployment zone was expected to be in the bay of Kiel, at a depth of about 10 m, which makes possible to avoid a 3-D array by neglecting elevation estimations and allowing the system to only focus on azimuth angles. As a result, a planar array was decided to be more suitable for the expected conditions.

Figure 24 shows a model of one of the hydrophones expected to employ in the hydroacoustics measurement system.

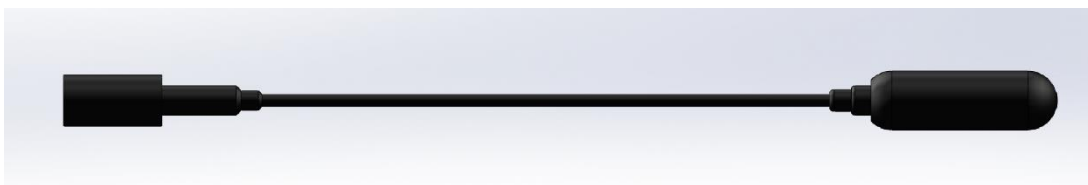


Figure 24. Modeling of hydrophone

To define the first design constraint, it was noticed that the dimensions of the hydrophones were fixed and limited by their cable length ( $23\text{ cm} \pm 1\text{ mm}$ ); therefore, the proposed array must consider this distance as one of the main design parameters. Considering this, to allow the detection of frequencies as close as possible to the 1 kHz band, the first design condition was to maximize the distance between the hydrophones. As a second condition, the array must be rigid enough to avoid deformations or distortions due to sea currents, because local or global movements of the array, even small ones, might cause great disturbances in the delays' calculations. Next, the array must be easy to build and assemble, and detachable. Based on the exposed design requirements, three proposals were considered to design the measurement system and all of them were based on a bottom/mounted configuration to avoid rotation and displacement due to water currents.

Hence, Figure 25 illustrates three array proposals.

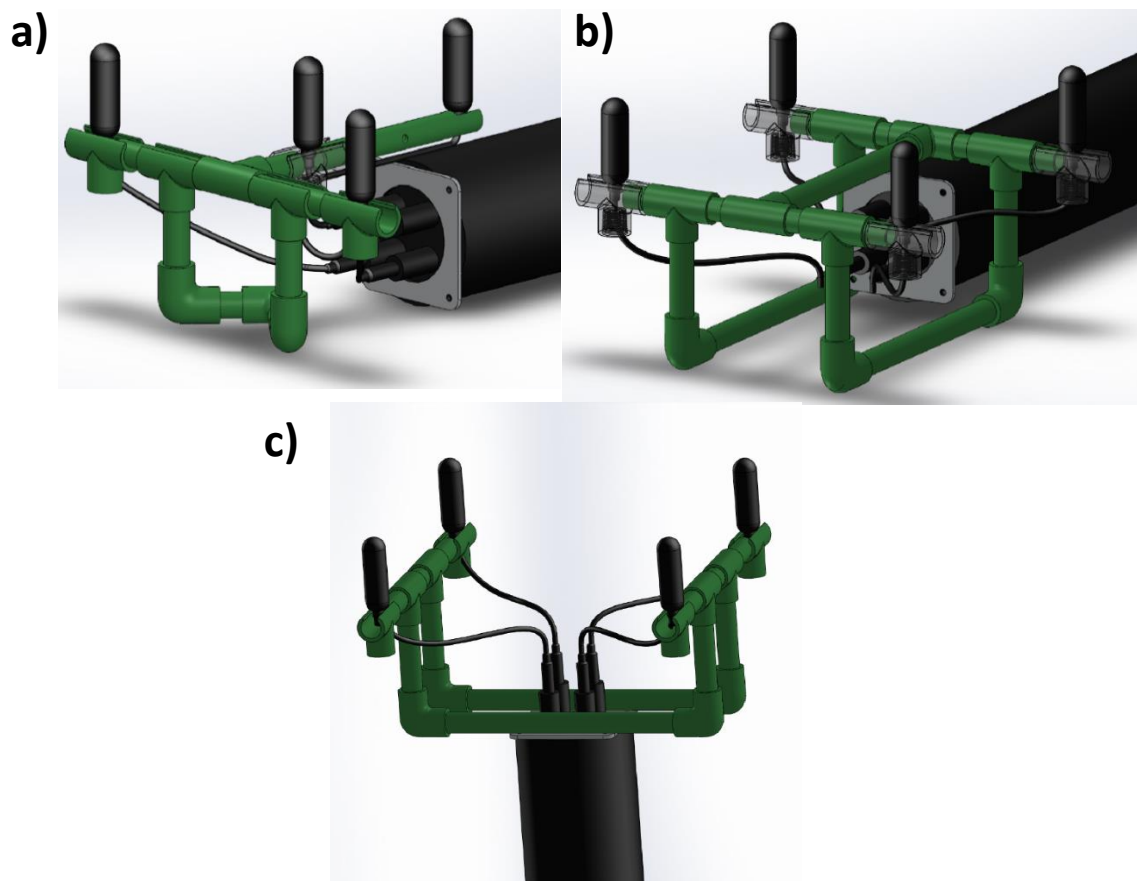


Figure 25. a) Triangular array. Proposal design 1. b) Horizontal Squared Array. Proposal design 2. c) Vertical Squared Array. Proposal design 3

Figure 25.a. shows a triangular array in a horizontal position, connected to the recorder, which was expected to keep the hydrophones in the right position. To build the main array structure it was proposed to use PVC or Polypropylene pipes and fittings, because of their low costs and they are common products in the market. Furthermore, they are rigid enough for the scope of the test. This proposal estimated a design frequency of 4.32 kHz, from the dimensions sketched in Figure 27.

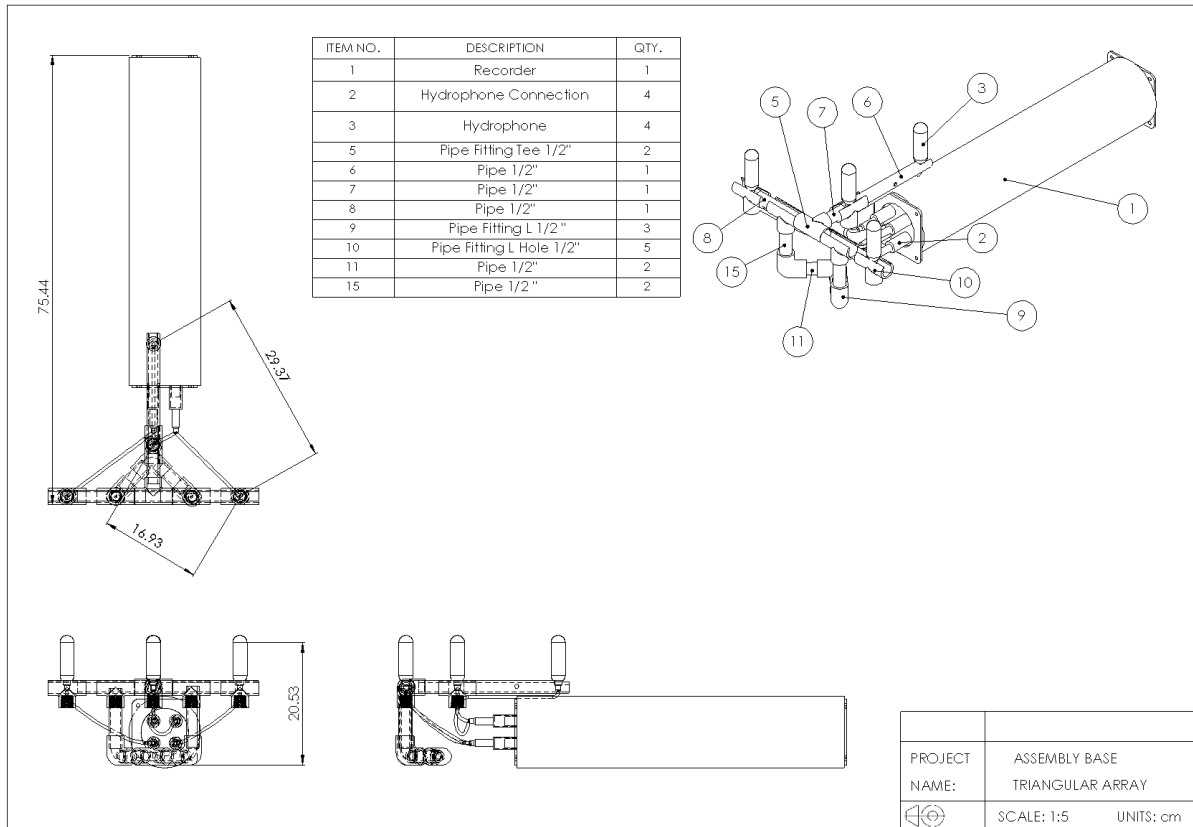


Figure 26. Proposal 1 sketch

Similarly, Figure 25.b shows the array in a horizontal position once is deployed, but this proposal considers a squared array instead of a triangular one. The solution shares the same idea as the previous array about reducing the center of gravity of the system as much as possible to ease a stable equilibrium in 5 degrees of freedom. The remaining dof was the rotation of the recorder around its longitudinal axis, which was initially planned to be solved by adding fixing equipment to make the surface in contact with seabed flat. For this proposal, the design frequency obtained was estimated in 2.36 kHz (Figure 27).

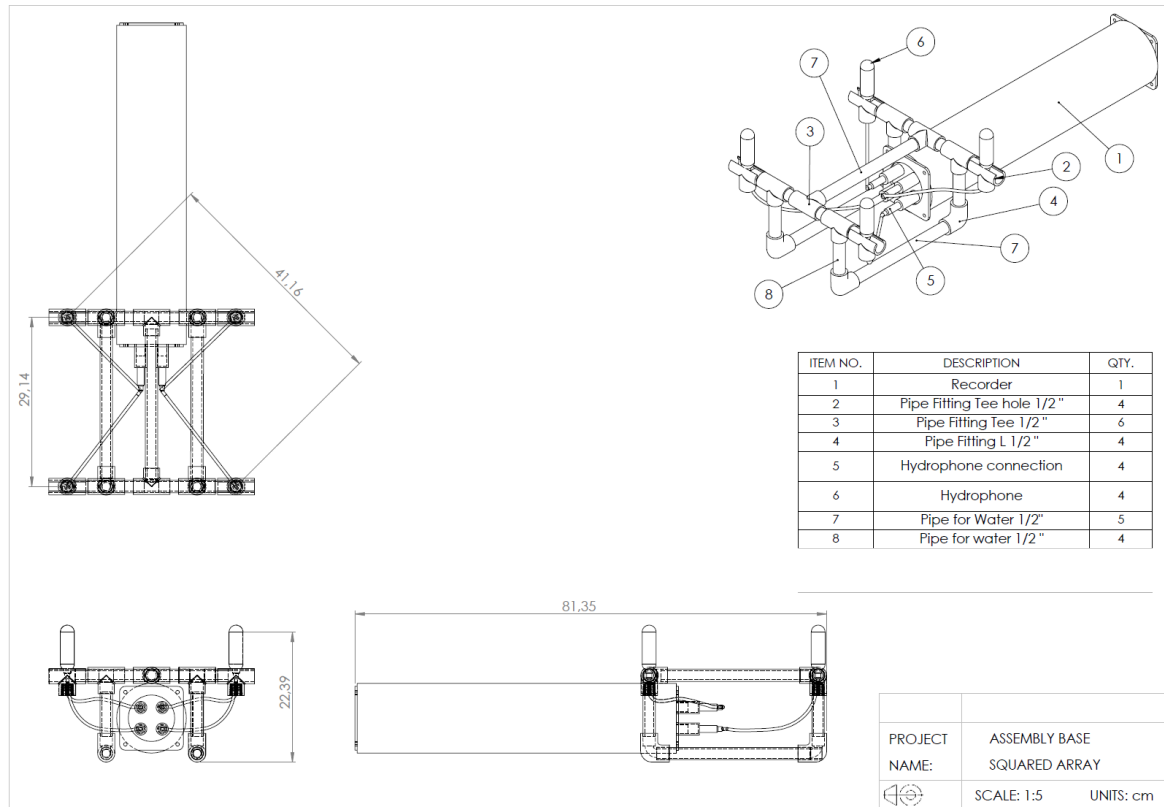


Figure 27. Proposal 2 sketch

The last proposal was based on a squared array, similar to proposal 2, but considering the array in a vertical position to increase even more the separation of the microphones to each other despite increasing the center of gravity. This solution provided a design frequency of 2.51 kHz, which was the best overall of the considered proposals, even though it is expected to be less stable once is deployed.

To make a proper decision about the more suitable design, it was considered a decision matrix as shown in Table 6.

Table 6. Array design decision matrix

Design Parameter	Horizontal Triangular Array	Horizontal Squared Array	Vertical Squared Array
Design Frequency (5)	1	4	5
Fixing equipment (4)	2	2	4
Low Center of Gravity (2)	2	2	1
Total	5	8	10

Given the advantages and disadvantages mentioned for each proposal and the decision matrix results, the vertical squared array was chosen as the definite proposal, keeping the maximum design frequency as the most important parameter, and the low center of gravity as the less



relevant. To overcome the dof constraint in this solution, a tripod device was implemented. In Figure 28, it is observed a model of the selected proposal.



Figure 28. Final proposal for measurement design

As was mentioned before, the main issue of this proposal was the center of gravity, which was solved by including counterweights in the tripod legs heavy enough to make it stable, though without deforming the system.

### 3.3. 4-Hydrophones Planar Squared Array Building Stage

In the previous section, it was selected an easy-to-build and simple proposal for the hydroacoustics measurement system. While the design process involved modeling and selecting the most suitable solution for the environmental conditions while keeping the hydrophones and the recorder safe. The building stage was focused on finding the material and tools to solve the issues that were not seen in the design stage.

In Table 7, is listed the materials required to build the array, without considering the tripod, counterweights, working tools and other accessories, that were provided by DW-ShipConsult; nor the recorder and hydrophones, provided by *Deutsches Meeresmuseum Stralsund*.

Table 7. Material list for the array construction

Material	N° of parts
Polypropylene Pipe Fitting, Tee (DN20)	4
Polypropylene Pipe Fitting, 90° Elbow (DN20)	4
Tee Pipe Insulation, Polyethylene Foam	4
Polypropylene Pipe (2m)	1
Threaded bar 1 m	1
M8 Hexagonal Screw	4
M8 Hexagonal Nut	4

During the construction stage, it was found two important problems, not taken into account in the previous section. The first one was a reference angle to deploy the system on the water. This is particularly important because even if the measurement system does not move, the bearing calculation needs a reference to compare with absolute coordinates and then properly compare with the results. In addition, the reference bar should help to align the array to a desired direction (if it is the case) and must be easy to check before, during, and after the system deployment.

The second parameter to consider was the deployment of the system to avoid internal movement and keep the recording devices safe. For this issue, it was proposed a deployment based on the sailing boat crane to lift the system up from the boat, rotate it and place it over the water surface, and finally slowly lower it to the seabed.

The two problems discussed above were focused on the deployment step of the system, although it is worth mentioning that aside those, the initial proposal solution worked well enough including an apparent stability and rigidity of the array.

In the next section, the deployment and testing process of the measurement system is described.

### 3.4. 4-Hydrophones Planar Squared Array Testing Stage

The testing of the proposed system was deployed in the Bay of Kiel, on May 31, 2022. Figure 29 shows the final assembly of the proposed measurement system before it was deployed on water. As can be observed, the solutions to the issues found during the building stage and some extra were implemented. Furthermore, to keep the system visible for other ships and recovering purposes, two reference buoys were fixed to the system. The position was approximately at the coordinate's 54°24'34.8"N 10°11'40.3"E, at 7.8 m depth.

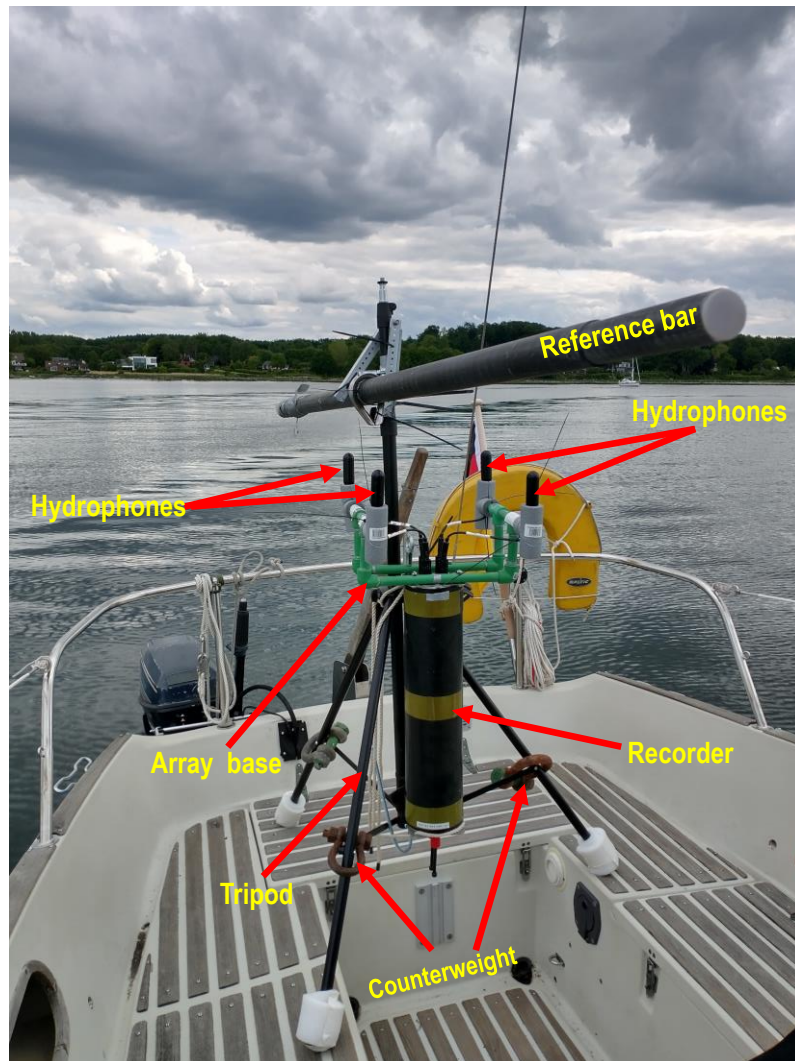


Figure 29. Array Assembled

Figure 29, also shows the angle reference bar fixed to the array. During the deployment, the system was aligned with the vessel, as it is illustrated in Figure 30, and the bow of the boat was aligned with a compass (Figure 31), thus, the bearing obtained from the recorded data was easily related to absolute direction by using an angle correction factor.

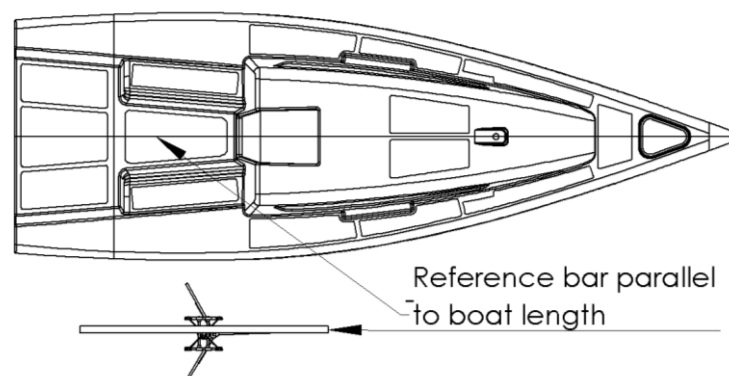


Figure 30. Deployment scheme

Figure 31 also shows the deployment of system and the reference buoys discussed previously.



Figure 31. Compass for reference angle (left) and deployment of the array (right)

Once the system was in position, and after around 2 minutes of waiting to record underwater background noise, the sailing boat started moving around the zone at different speeds. Additionally, during the time in the sailing boat, it was observed the presence of different ships (big, mid, and small-sized) passing nearby the recording zone and for most of them, it was registered the passing time, the characteristics and the number of them.

In Figure 32, is detailed the sailing route accomplished in about 1:30 hours and the position of the array. The idea behind the target traveling at several angles and different distances respect to the array, allowed it to evaluate the performance of the design system in several cases.

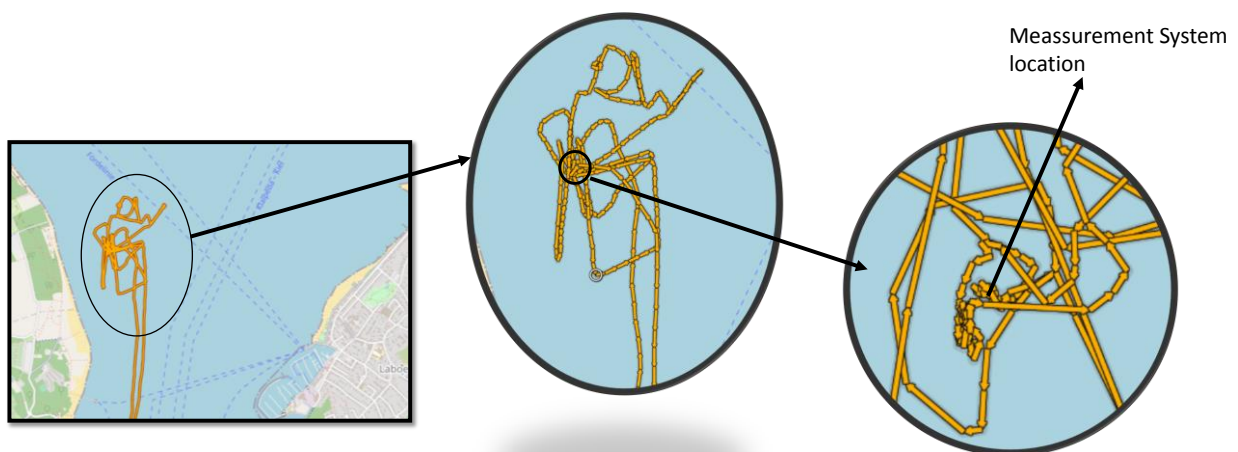


Figure 32. Sailing route description

## 4. RESULTS AND ANALYSIS

This chapter describes the bearing estimating process for the concerned sources (target boat and additional ships), starting from the recorded data processing to the bearings calculations. The signal processing included extraction of valid data, signal filtering, SNR calculation and analysis of cross-correlation plots. Besides, GPS data from the main sailing boat was extracted to validate the actual bearings respect to the estimated with the proposed DOA model. Finally, the results are discussed.

### 4.1. Acoustic Data Processing

A preliminary step to processing the acoustic data recorded by the measurement system, involved the extraction of the ship bearing from the GPX file. To get this information, the data was filtered between 16:13:00 and 17:51:00 CET (Central European Time), defined as starting and finish recording time, which included more than 200 discrete times with their respective bearing details.

Moreover, during the recording phase, two more big ships were passing by, and it was possible to access to their positioning information through (Marine Traffic). In particular, this kind of ships is out the scope of this research and the design system itself, but their positioning information in time was used to verify whether the bearing of the main target was affected by the proximity of these ships to the measurement system. In Figure 33, it is shown part of the shipping route from the mentioned ships during the recording phase.

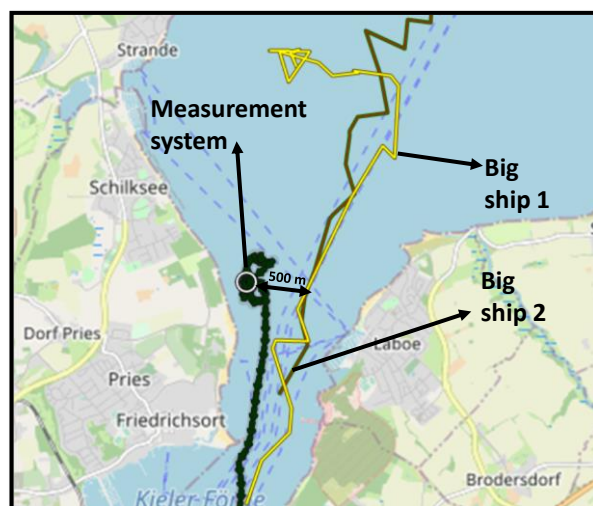


Figure 33. Maritime route of two big ships in recording zone



The recording data processing was carried out by determining a suitable time window of background noise before starting the sailing boat engine. Figure 34 shows the recorded signal during the last minutes of the system deployment and the time the main target started to move away. Since this background noise was used to evaluate sound-to-noise ratio values for the whole data, it is worth mentioning that this approach is not ideal regarding the dependency of background noise on live shipping traffic, therefore, this assumption has some intrinsic inaccuracies on it. However, despite the errors this approach might carry to the results discussion, it is a practical way to rate possible signal masking issues during the recording.

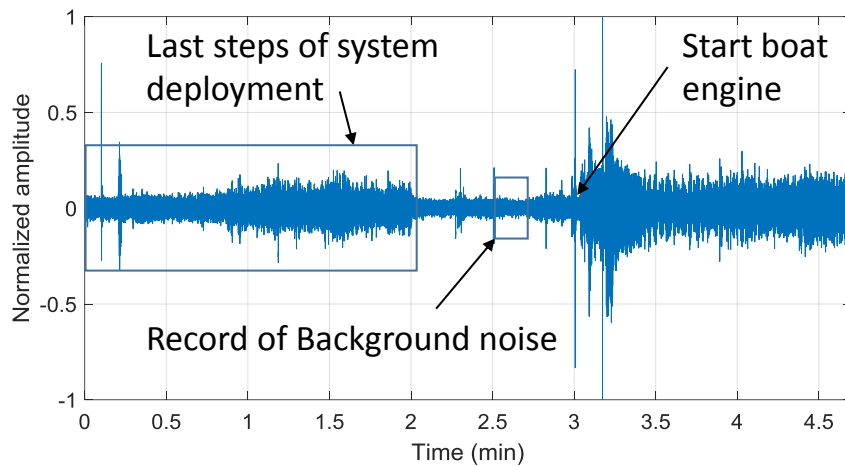


Figure 34. Background noise sample

Later on, it proceeded to verify the detection of sources from the recording data by using a time-frequency diagram detailed in Figure 35. As can be noticed, x-axis (time) has two tick labels; the horizontal one represents the absolute time from the  $t=0$  to  $t=1:15$  h and the vertical label represents the time in Central Europe (CET). To detect the targets, it was detailed the variations in frequency that in most cases, were found between 500 Hz-2500 Hz, with increases and decreases that were related to how strong the signals were received by the hydrophones when the sailing boat was closer or farther to the measurement system.

Moreover, by mere observation of the spectrogram, some hypotheses can be made relating the times when frequency changes occurred with the registered times from the vessels that were passing nearby.

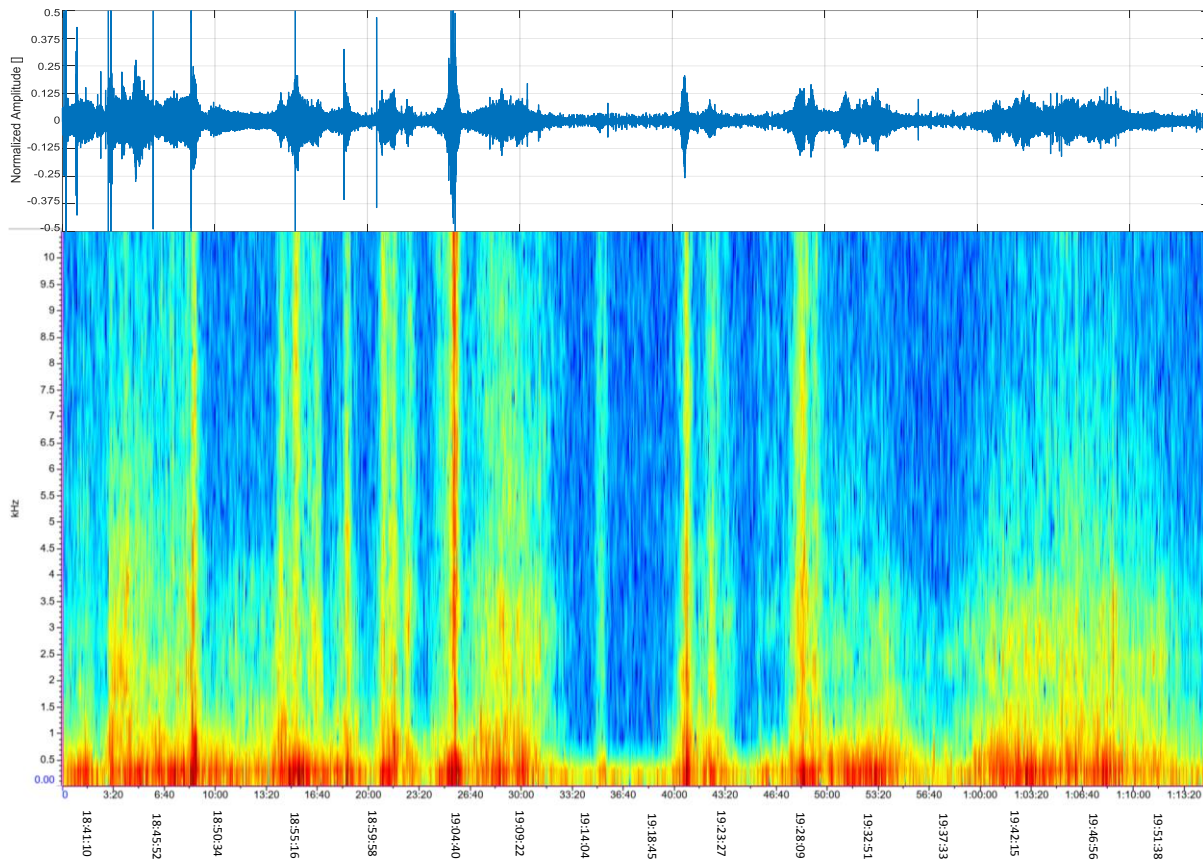


Figure 35. Recorded time spectrogram

For instance, in [30:10-40:00] min range, the decrease of radiated noise from the target ship is evident, which was associated with the sailing boat being out of measurement range of the system, or sounds transmission losses were more relevant during this period. Another preliminary observation from Figure 35 is an almost flat and smooth behavior during the last 15 minutes with no drastic changes in frequency, maybe due to the dominance of the one source moving but at relatively constant distance from the array.

To provide a deeper analysis, Figure 36 shows the spectrogram including the registered information from the observed ships.

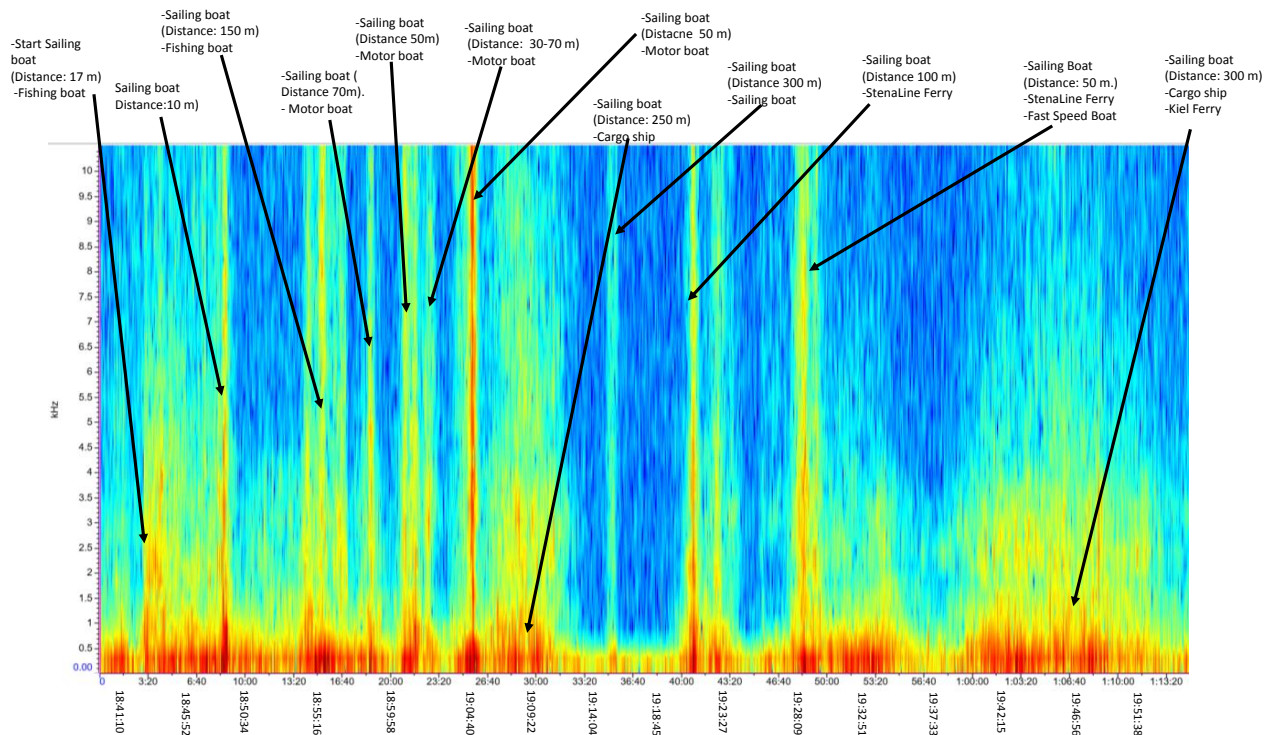


Figure 36. Identification of sources in spectrogram

The first section of Figure 36 includes changes in frequency after about 3 minutes that coincide with starting of the engine of the target boat and in frequencies in the order of 2 kHz; close enough to the design frequency of the array. Later on, it was noticed a smooth decrease in the frequency at the time a fishing boat was moving away from the measurement system.

In minute 8, it is observed again a frequency increase, along with an apparent out-of-detection range of the fishing boat and the sailing motor boat getting closer to the array. In the same order of ideas, between minutes 9 and 13, the frequency behaved in a constant way close to 1 kHz, while the sailing boat is around 150 m away from the recorder. Since all changes in amplitudes were assumed two important things:

- The detection of the main target when is approaching or getting farther from the array.
- The detection of other ship passing by the recording zone.

Considering the last statement, the previous preliminary analysis can be easily extrapolated to the rest of the signal considering the identification arrows at the top of Figure 36.



## 4.2. Bearing Calculations

Continuing with the evaluation of the recording, it was split up into the total number of discrete times presented in the GPX file, which allowed improve the audio reading and focus with ease on the time ranges of concern. Then, it was applied a band filter in the band [2250-2650] Hz to each one of the sample cuts and proceeded with the bearing calculation. Figure 37 shows the scheme of the algorithm proposed to estimate the azimuths.

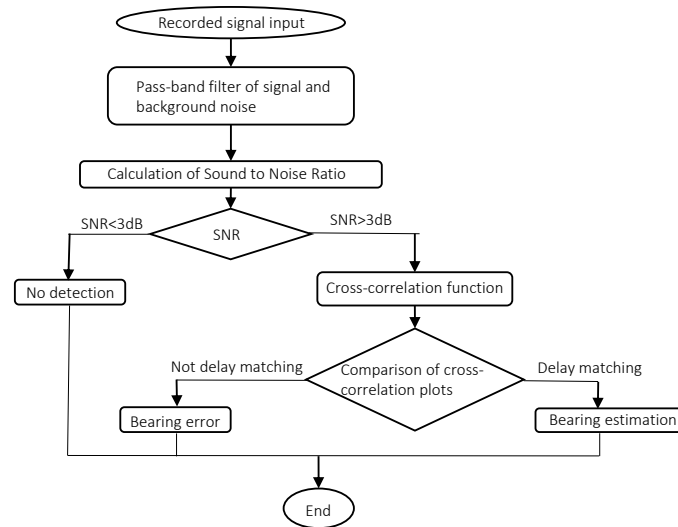


Figure 37. DOA model algorithm scheme

The proposed routine had as input the four hydrophones signals and the threshold defined for the cross-correlation functions. The outputs are the bearing and number of sources. Concerning Figure 37, SNR values were evaluated to decide whether the calculated bearing should be taken into account or not, because low SNR values, affect time delay difference estimations (Chuanqi, et al., 2021). Once the low SNR values were filtered from the original data, Figure 38 shows the SNR distribution per hydrophone. Interestingly, SNR distributions from all hydrophones are not the same, nevertheless, most of the SNR values were between 12 and 18 dB, which means that most of the bearing were calculated using signals from 10 to almost 100 times higher than the ambient noise.

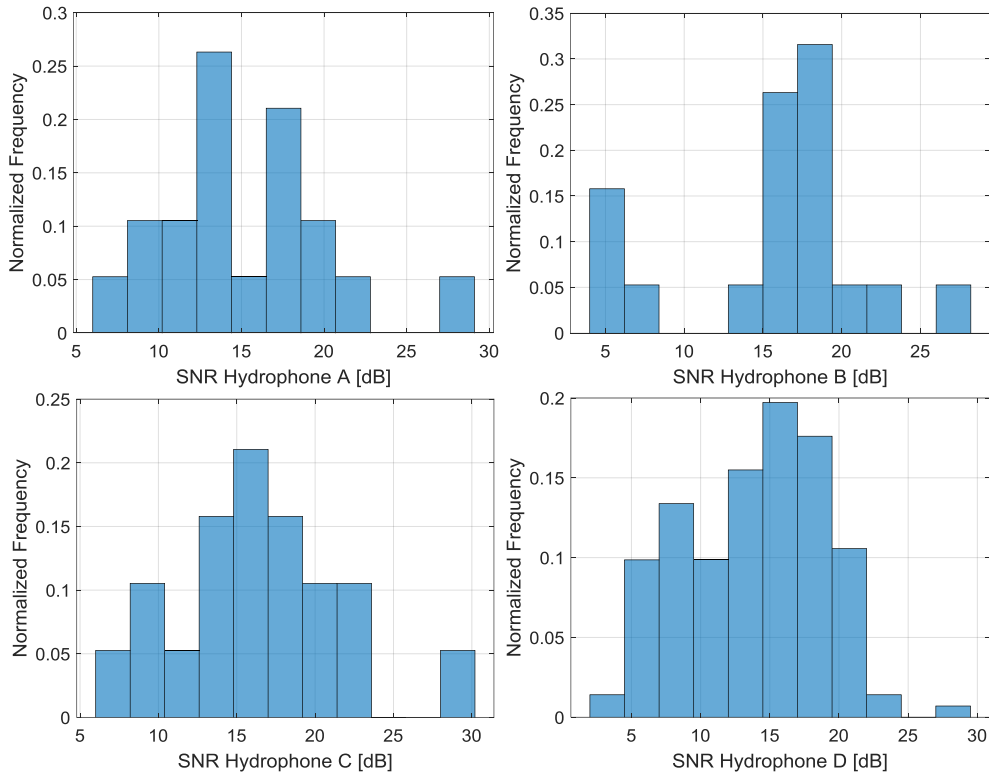


Figure 38. Histogram of SNR values per hydrophone

Aside from SNR values, another source of error in bearing calculation come from finding the right peak from the cross-correlation function, even if no signal masking problems is observed. The last statement goes along with the possibility to apply an extra verification during calculations. When dealing with a planar array, three hydrophones are enough for a bearing estimation without ambiguities, although, extra hydrophones open the possibility of making bearing verification, in this case, three bearing matching were carried out instead of two (minimum requirement).

These three bearing comparisons, allowed improving the quality of the results, specifically in cases where more than one source was present. Figure 39 shows different cross-correlation functions where more than one source was expected, although, as can be noticed, identifying sources is not always evident just by simple inspection. An extra delay allows the routine to estimate additional angles of arrival to match the ones not completely confirmed as solutions and reduce the detection of phantom sources.

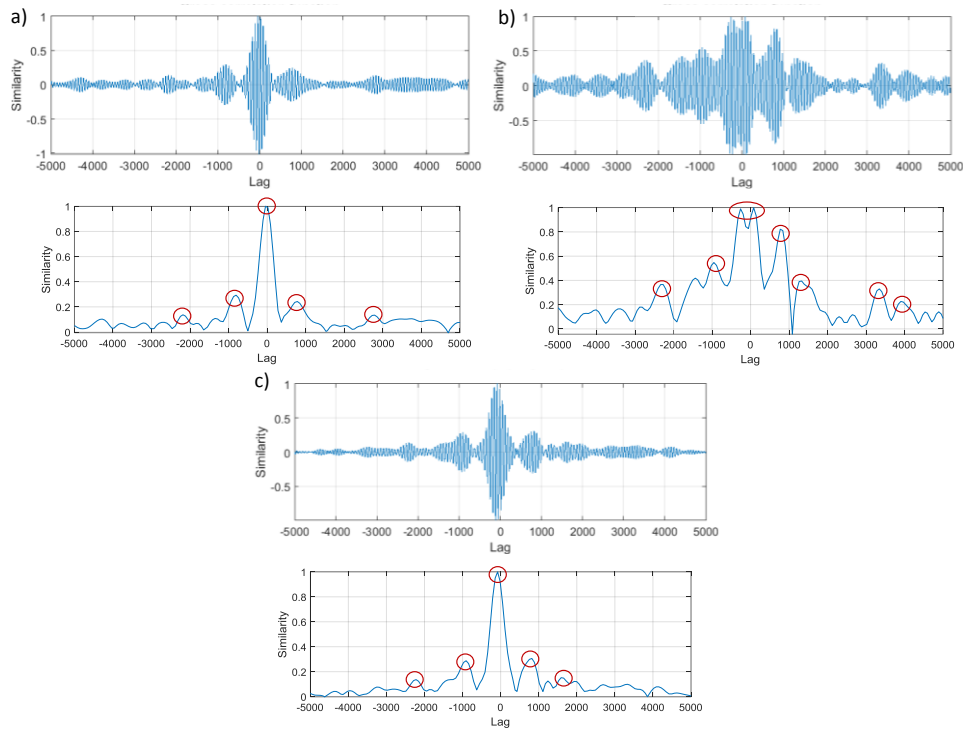


Figure 39. Cross-correlation function. a) Hydrophones A-B, b) Hydrophones A-C and c) Hydrophones A-D

In Figure 40, the bearings estimated from the sailing motor boat are compared to the real angles with respect to the GPX data. Bearing distribution over time shows a good approximation and a similar behavior for most of the considered cases.

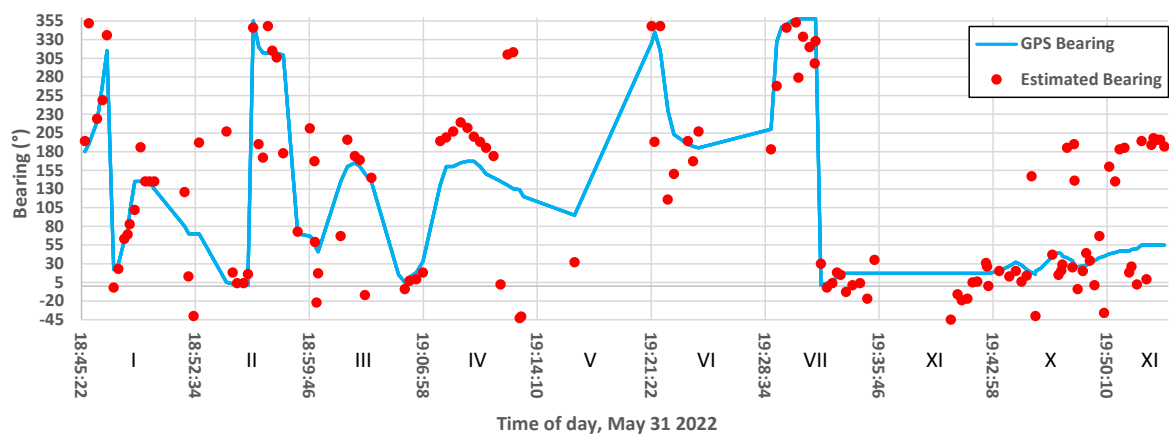


Figure 40. Estimated bearing (azimuth) compared to GPS data

Moreover, Figure 41 shows the boat distance from the array during the recording time, estimated from the sailing boat GPS information and the location of the measurement system.

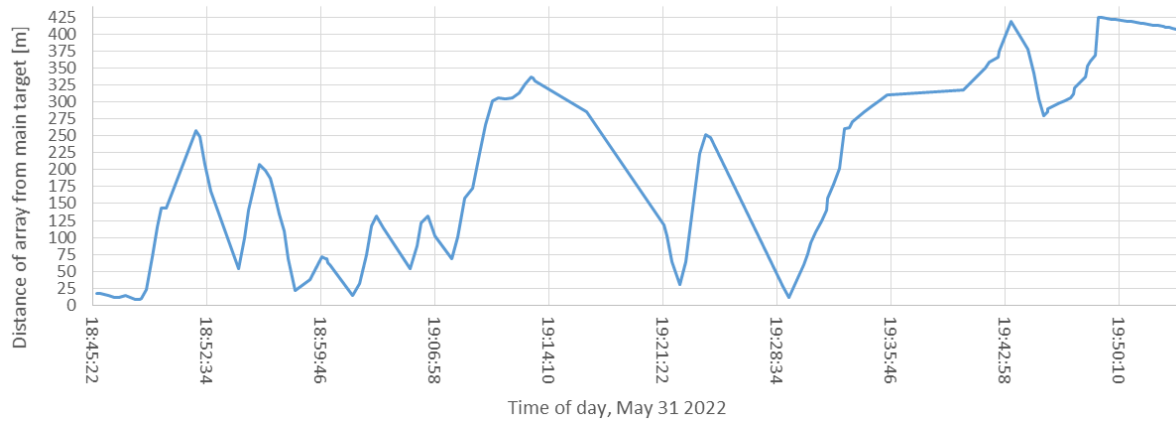


Figure 41. Separation distance array-Sailing boat in time

Interestingly, the results show a better approximation to actual bearings during some time ranges than others. To accomplish a more detail analysis of local results, the time axis was divided into 10 sections (Figure 40).

Section I covers 19 bearings where their absolute errors were plotted in the histogram represented in Figure 42, showing 42% of the bearing errors below  $20^\circ$  and 21% between  $20^\circ$  and  $40^\circ$ . The rest of the bearing errors were found below 10% distributed between  $[40-180]^\circ$ . Furthermore, from Figure 41 the mean distance from the array to the boat was 125 m, which according to the obtained results, this distance seems that is not a factor that affects bearing estimations.

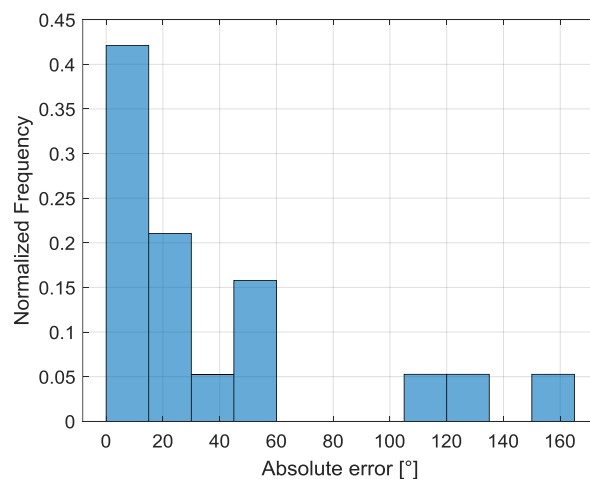


Figure 42. Bearing error histogram Section I

Continuing with the bearing histograms, from sections II (Figure 43), were covered 13 bearings with 61% of them with errors below  $20^\circ$  and 15% were found between  $114^\circ$  and  $133^\circ$ . This time, the boat navigated at similar distances than the previous case, and the bearings shows also a good approximation to the actual values. Then, the same figure shows the histogram of

section III where 58% of errors are below  $17^\circ$  and 17% in  $[68-85]^\circ$  range, considering 12 bearings.

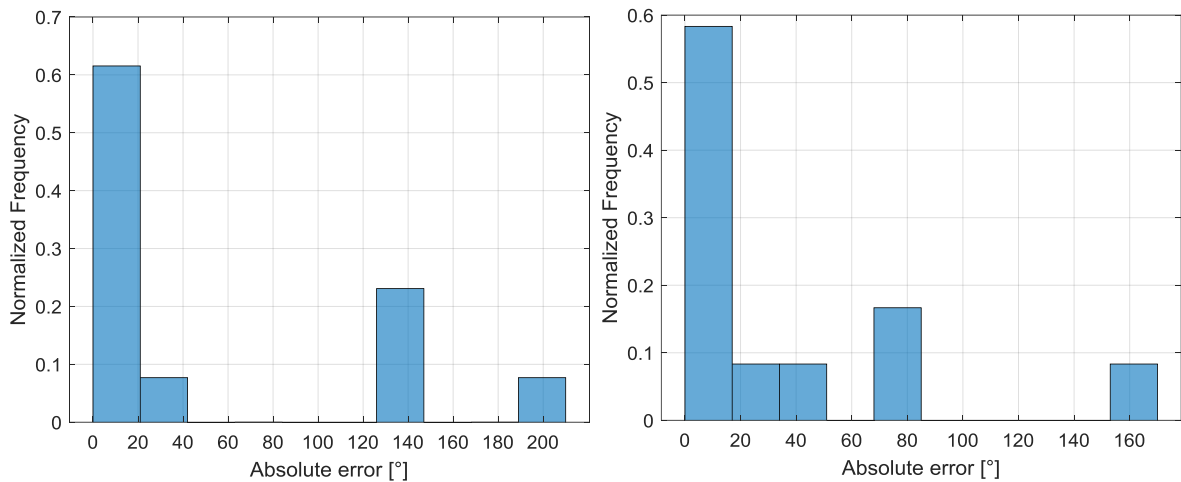


Figure 43. Bearing error histograms of section II (left) & section III (right)

Histograms from Section IV and VI are represented in Figure 44. For the first one, 26% of bearing errors were between the ranges,  $20^\circ$ - $40^\circ$ ,  $40^\circ$ - $60^\circ$  and  $172^\circ$ - $192^\circ$ . Contrary to the results from the previous sections, in this one, the bearings error do not show a clear tendency since are distributed in three different ranges. During this section, the maximum distance from the ship was about 325 m, which is expected to be the reason for the poor bearing detection. Since an out-of-range problem is plausible considering also the spectrogram from Figure 36 and the important decreases in the frequency and strength of the signal at certain ranges.

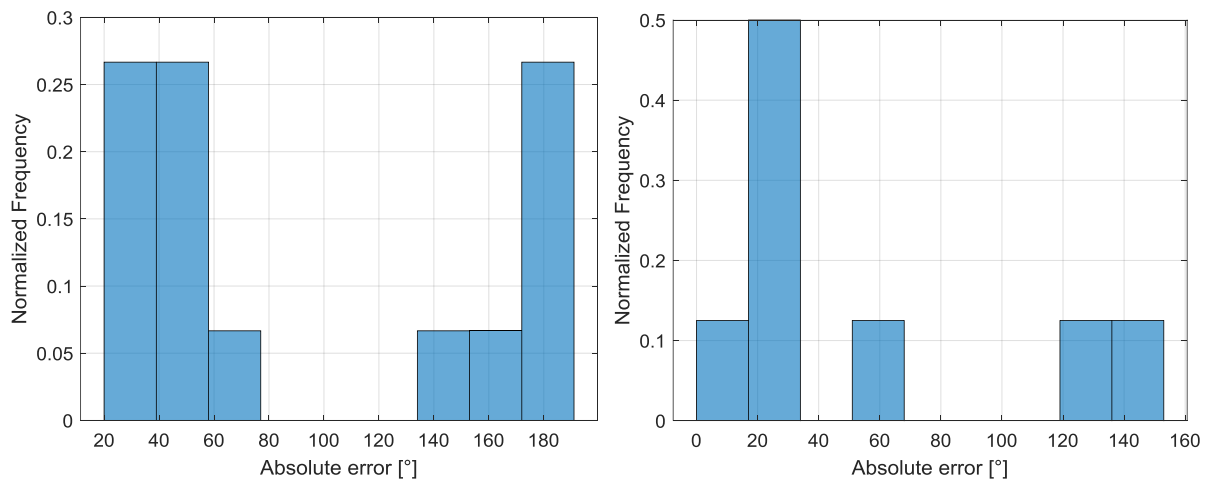


Figure 44. Bearing error histograms of section IV (left) & section VI (right)

Furthermore, to support the previous statement, in section V were found high errors and only a few values from the original data in this section had suitable SNR values. However, at the end of this section, the boat approached to the array and as is detailed in the histogram for section

VI, bearing accuracy improved. In section VI, 8 bearings were considered, and 50% of errors were smaller than  $17^\circ$  and 13% between  $17^\circ$  and  $34^\circ$ .

Section VII and VIII (Figure 45) show similar behavior in their error histogram despite considering a very different amount of data. For the first one, 39% of the error were below  $17^\circ$  and 32% in  $17^\circ$ - $34^\circ$  range and 10% between  $51^\circ$  and  $60^\circ$ , with 28 total angles. In addition, notice that in this section the boat started getting away from the array in an approximate linear behavior (Figure 41) until reaches a distance of 300 m. However, notice that there were no important decreases in frequency in the spectrogram (Figure 36), as was observed in sections IV and V. This is justified by the presence of other ships (big and fast boats), which were supposed to keep high the strength of signal even if the main target was not within recording range.

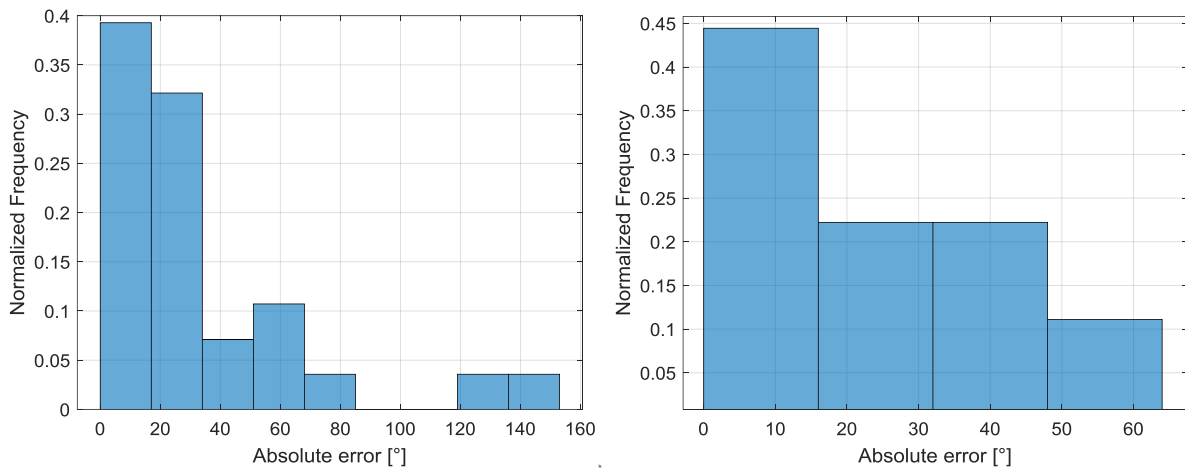


Figure 45. Bearing error histogram of section VII (left) & section VIII (right)

In Section VIII, were estimated 44% of bearings below  $16^\circ$  and 22% between  $17^\circ$ - $33^\circ$ . In addition, during this period, no error surpasses  $65^\circ$ .

The histogram of absolute error found in section IX is detailed in Figure 46, with distribution lower than  $20^\circ$  at 40% of the time and 22% of errors between  $21^\circ$  and  $40^\circ$ . During this period, it is worth noticing that the mean distance of the sailing boat from the array was 350 m, but over 27 estimated bearings, only 11% got error between  $120^\circ$  and  $140^\circ$ . However, less accurate results were found when the distance array-boat was longer than 350 m. Besides, the accuracy in section X were poor, with 57% of the error between  $128^\circ$ - $146^\circ$ , but also the boat was located close to 400 m away from the hydrophones array.

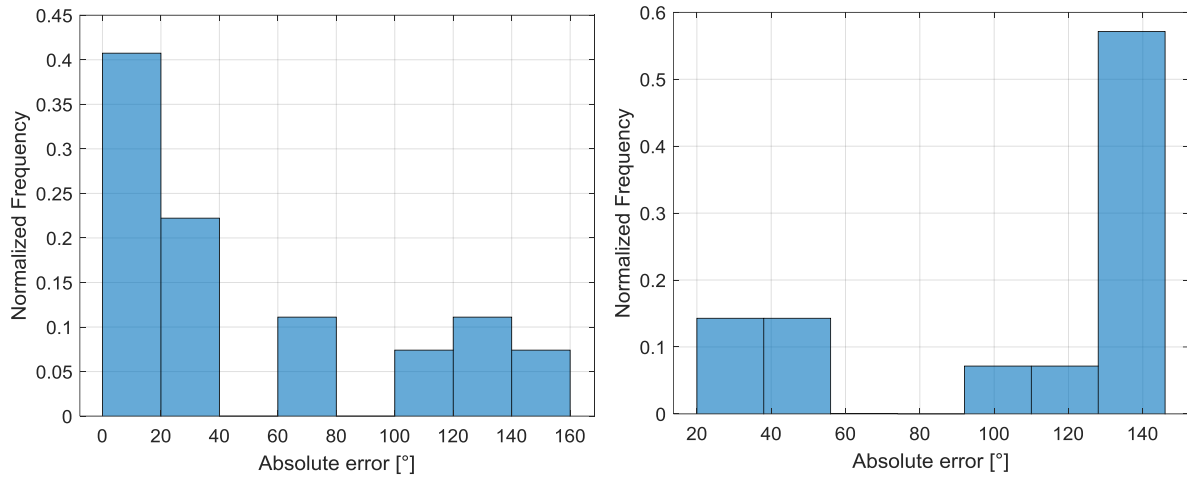


Figure 46. Bearing error histogram of section IX (left) & section X (right)

Finally, the overall bearing results are summarized in Figure 47, where 37% of absolute errors were below 20°, 23% between 21°- 42°, and 10% for both [43-64]° and [106-147]° ranges. The rest of the errors were below 5%.

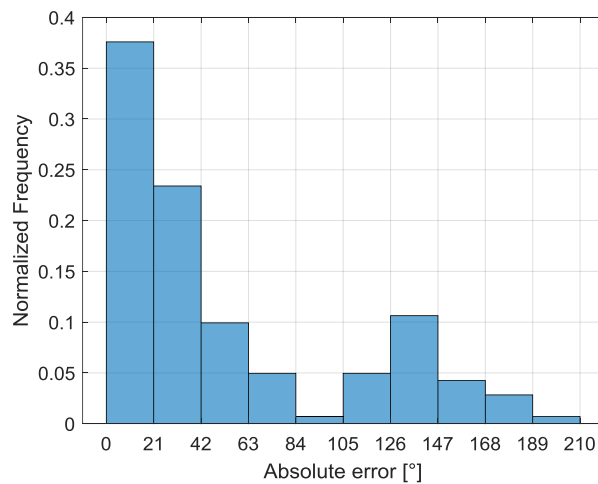










Figure 47. Overall bearing error histogram

The evaluation of the bearing errors distribution shows there is a relation between the distances from the main source to the measurement system, supported by the fact that for longer distances than 325 m, results decrease drastically in accuracy, even the cases when SNR values showed good signal qualities. The last statement aimed to presume that during those periods, background noise gained relevance that was not considered into SNR calculations. Finally, table 8 shows the ships registered during the recording period and the estimated bearing as well as the calculated.

Table 8. List of ships registered during the experiment

CET Time [h:m:s]	Ships	Approximated bearing [°]	Calculated bearing [°]	Error [°]
18:45:52	Fishing boat	225	238	13
18:50:34	Fishing boat	45	10	35
18:53:00	Sailing boat	45	27	22
18:55:00			23	22
18:55:16		70	90	20
18:56:00	Sailing boat	45	34	11
18:57:00	Sailing boat		242	197
18:59:58	Sailing boat		63, 30 & 19	18
19:02:00	Sailing boat	270	34	11
19:03:00	Sailing boat		242	28
19:04:40	Sailing boat		290	20
19:05:00	Sailing boat		290	20
19:09:00		0	23 & 11	11
19:09:22	Sailing boat	180	11 & 217	37
19:13:00		225	239 & 273	14
19:14:00	Sailing boats	45	Low SNR	--
19:14:04				--
19:18:46				--
19:22:00		135	114	21
19:26:00		15	37	22
19:32:52	Sailing boat	180	226	46
19:37:00	Ferry	90	SNR low	--
19:37:34	Sailing boat	0		--
19:38:00	Container	135		--
19:42:16	Sailing boat	90	60	30
19:43:00		135	31 & 210	75
19:46:58		135	297	162
19:49:00		135	90	45
19:51:40	Sailing boat	90	90 & 281	0



Taking into account the extra sources passing by during the recording, passing time and the kind of vessel were directly registered. However, for bearings approximations were made considering the position at which each ship was seen, a compass and a reference map with the measurement system in position as is observed in Figure 48.

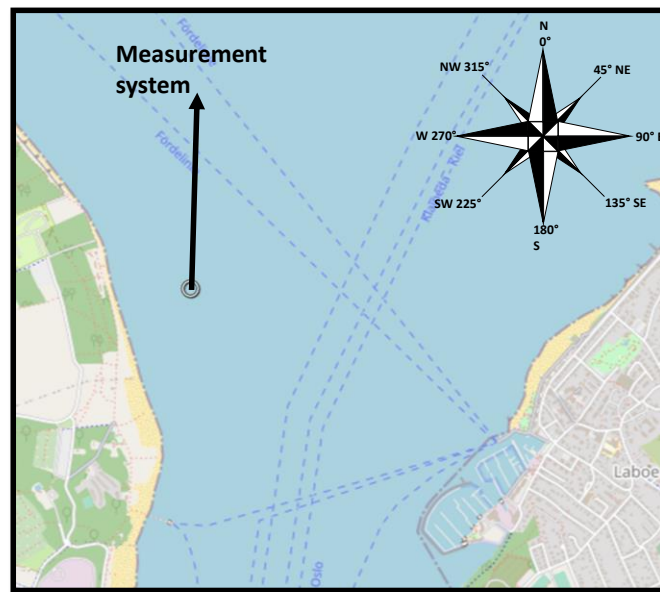


Figure 48. Bearing reference to recording zone

From Table 8 it worth to notice that in some cases the number of sources were wrongly estimated (indicated by more than one angle) but two important facts need to be kept in mind with the bearing estimation for several sources. First, two or more sources at similar bearing are counted as one, but with a good bearing estimation. Second, when there is one extra source and the DOA model shows several, although, they are relatively close one to another. Fortunately, the second scenario can be overcome by improving the matching of bearings, but more details of the position of the extra source are required for a proper validation.

Finally, in addition to the information from Table 8, Figure 49 shows the spectrum of the sailing boat recorded around minutes 41-42 (Figure 35). In this case, to compare with the background noise, it was considered a windows starting at minute 40 (where the measurement system was not detecting the boat), this allowed to have a more precise comparison because the signal and ambient noise had only few minutes of difference of being recorded. Furthermore, it allowed to detailing more properly the acoustic emission from the sailing boat.

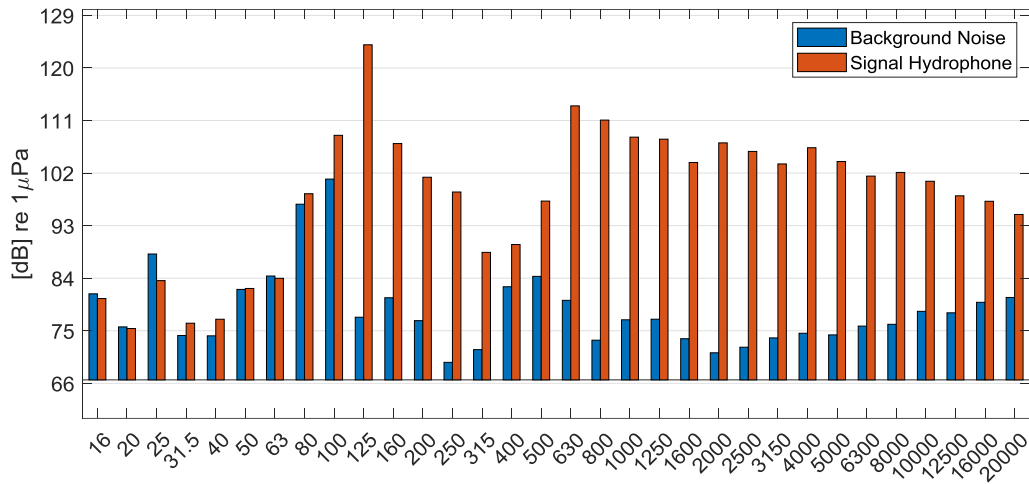


Figure 49. One-Third octave spectrum (Sailing boat)

Figure 49 illustrates that the system is able to detect the signal of the boat under the right circumstances (inside a measurement range). Moreover, it is evident that the background noise has no relevant amplitude in comparison with the ship signal for high frequency bands. Besides, it is important to remember that the frequency of interest (design frequency) is within the band 2500 Hz, which as can be detailed has a difference respect the background noise of almost 30 dB.

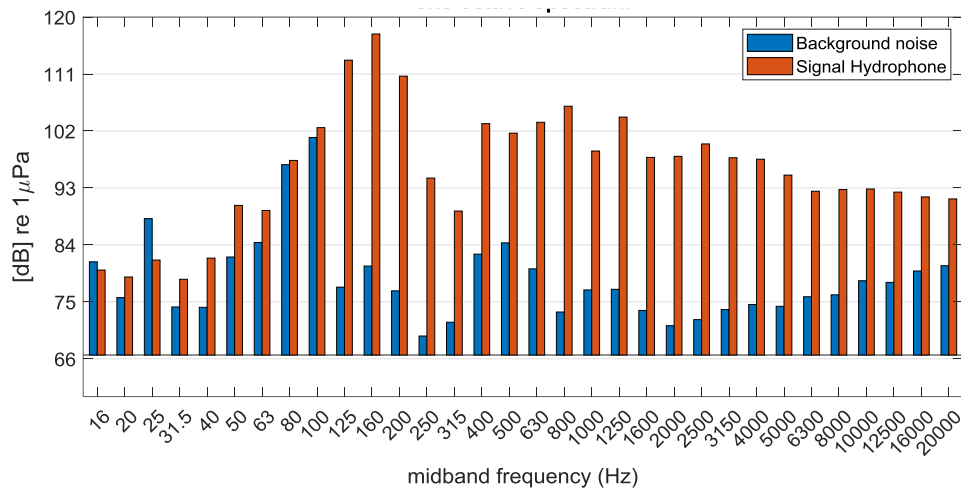


Figure 50. One-Third octave spectrum (fast boat, Ferry and Sailing boat)

Figure 50 shows the spectrum around minute 48 where a fast boat, the Stena-Line ferry were passing by and the sailing boat was at around 50 m from the recording system. In comparison with the previous spectrum in this case there are not relevant changes in the level distribution, except for the increase in the amplitudes in the 400 and 500 Hz frequency bands, which is expected to be related to the Ferry radiated noise, nevertheless, due to the distance from the

measurement system and the contribution to the motor boat and the sailing boat signals, both of them closer to the array, their contribution to the signal is more relevant.

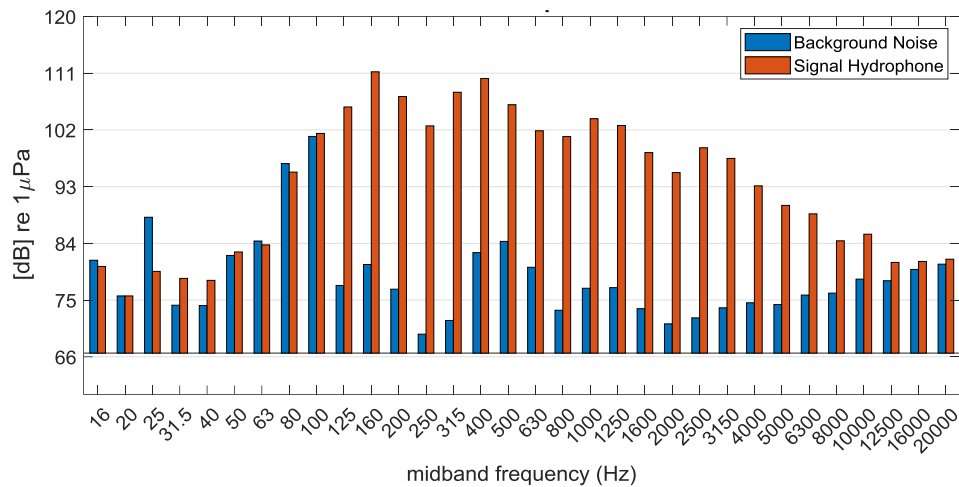


Figure 51. One-Third octave spectrum (SKF Ferry)

Figure 51 represents the moment a SKF ferry (Kiel local ferry) was passing by and the sailing boat was about 250-300 m from the measurement system. In this case, notice that in comparison with Figure 49, the high frequencies lost relevance. Furthermore, frequencies around 400 Hz band are in this case higher than in the sailing boat spectrum.

The spectrums from the last two cases are not as evident as the initial sailing boat spectrum from Figure 49, because the contribution of other sources. However, by noticing that there are changes in a reference spectrum such as the sailing boat (in this case) or background noise, it is possible to estimate that new sources are contributing to the signal. Moreover, with the spectra and the right information about the expected sources it can be predicted which kind of vessel is being recorded.

## 5. CONCLUSIONS

In this thesis, a system to investigate underwater radiated noise of small craft was studied, designed, fabricated and tested in real hydroacoustics environment. It mainly focused on counting and bearing estimations for one and several sources, but it opened the possibility to perform more complex research.

Several schemes to estimate the position sources by acoustic means have been reviewed with especial emphasis on time delay-based methods. For most localization methods based on small dimension arrays, accuracy and equations solving, are a challenge that requires both, accurate instrumentation and proper numerical methods to aim for accurate bearing estimations.

Direction of arrival is a simple method for bearing estimation that offers several alternatives to estimate not only one but also several bearings from different sources at the same time.

The cross-correlation technique was successfully coupled to DOA basic algorithm to estimate bearings from different sources without result ambiguities by using 3 pairs of hydrophones signal comparison.

The proposed routine for bearing calculation was applied to underwater acoustic recordings, which covered the acoustic signatures of a motor sailing boat, carriers, a naval ship, ferries, sailing, fishing and fast motor boats in a shallow water condition environment. The routine based on the DOA method was applied to the detecting and bearing estimation of recreational craft, providing useful bearing estimation by achieving absolute errors lower than  $20^\circ$  in 37% and between  $21^\circ$  and  $42^\circ$  to 23% to the total data, respectively.

Bearing estimation of different sources by having a look at the cross-correlation function is not always evident, and with the wrong analysis, the wrong number of sources might be counted. Comparing the bearing obtained by different pairs of hydrophones bring the possibility to improve the accuracy in bearing estimations and thus the number of sources.

Underwater acoustic research requires suitable signal processing tools depending on the performance of a correct evaluation of the data. Furthermore, a combination of different signal processing tools allows to performing deeper analysis, depending on the scope of the intended work and the complexity of the phenomenon involved.

Evaluation of background noise is one of the first and the most important task to carry out, especially in detection applications, where false-positive results might be common. However, is not straightforward to have constant monitoring of this noise while doing the measurement for bearing estimation. However, for better background noise approximations, longer samples might be recorded at different dates and times, to improve the evaluation of signals quality.

Underwater acoustic recordings are complex to analyze without preliminary information regarding the condition and expected source to evaluate. Moreover, underwater noise pollution is a common factor that might distort the information of concern, if the right preprocessing practice is not applied, such as finding suitable time windows or applying the right filtering methodology.

Acoustic arrays must be designed considering different factors that may not be necessary all covered, therefore, decision techniques must be taken into account and assure the most critical requirements are satisfied.

Literature about hydroacoustics of recreational craft is nowadays limited and it is needed more work to overcome the current challenges in that field. This work shown, that a simple and cheap measurement configuration is possible to study phenomena like underwater acoustics at different levels of complexity.

## 6. ACKNOWLEDGEMENTS

This thesis became a reality with the kind support and help of many individuals, and I would like to extend my sincere thanks to all of them.

First, I would like to express my gratitude to Dietrich for his assistance, patience, time and the opportunity to be part of DW-ShipConsult. I also want to thank DW team, including Johanna for her time, effort and generosity to help me out with all my questions; Dorian for sharing his knowledge regarding signal processing and German language; Paul for his assistance during the whole testing of the system as well as taught and allowed me to steer his boat; Thomas, Max, Florian, Ronald, Felix, Bertina and Kurr, for creating a nice working environment and teach me a lot about German culture.

I wish also to thank The EMSHIP committee for providing all kinds of support during the last two years and bringing me the opportunity to meet interesting people that I can now call colleagues and friends. Specifically, I want to thank my fellows during my time in the University of Liège and the University of Rostock: Asib, Cherif, Pharindra, Sangeeth, Ammar, Bei-Jhen, Mikolaj, and Victor, for all the fun we had during the relaxing and stressful moments.

I am also very grateful to the Kiel Coast Guard Police, for towing the sailing boat used for the core of this project, and saving us from spending the night in the middle of the sea, already tired and with no extra food supplies, without your help, I do not know what would have happened.

Rosa and Julio, I wasn't there for you, but you were with me during this long journey... thank you.

## 7. REFERENCES

- Abraham, D. A. (2019). *Underwater Acoustic Signal Processing*. Ellicott City: Springer.
- ANSI. (2004). *ANSI S1.11: Specification for Octave, Half Octave, and third Octave Band Filter Sets*. Melville, NY: Acoustic Society of America.
- Arshad, M. R. (2009). Recent Advances in sensor technology for underwater applications. *Indian Journal of Marine Science*, 267-273.
- Arveson, P., & Vendittis, D. (2000). Radiated noise characteristics of a modern cargo ship. *The Journal of the Acoustical Society of America*, 118-129.
- Baron, V., Finez, A., Bouley, S., Fayet, F., Mars, J., & Nicolas, B. (2021). Hydrophone Array Optimization, Conception, and Validation for Localization of Acoustic Sources in Deep-Sea Mining. *IEEE Journal of Oceanic Engineering*. Retrieved from <https://hal.archives-ouvertes.fr/hal-03052568>
- Beyer, R. T. (1999). *Sounds of our times, two hundred years of acoustics*. New York: Springer Verlag and AIP Press.
- Buehrer, M., & Zekavat, S. (2012). *Handbook of Position Localization*. Singapore: IEEE Press.
- Chapra, S. (2007). *Métodos Numéricos para Ingenieros*. México: Mc Graw Hill.
- Chuanqi, Z., Shiliang, F., Qisong, W., Liang, A., Xinwei, L., & Hongli, C. (2021). A Time-Frequency Joint Time-Delay Difference Estimation Method for Signal Enhancement in the Distorted towed Hydrophone Array. *Remote Sensing MDPI*, 13.
- Coppens, A. B. (1981). Simple equations for the speed of sound in Neptunian waters. *J. Acoust. Soc. Am.*, 862-863.
- European Commssion. (2008). *European Parliament and the Implementation of the Marine Strategy Framework Directive*. Brussels: European Commission.
- Gloza, I. (2009). Ship's underwater noise measurements using sound intensity method.
- Hallander, J., & Johansson, T. (2015). Underwater radiated noise measurements on a chemical tanker. *4th Int'l Conference on Advanced Model Measurement Technology for the Maritime Industry (AMT'15)*. Istanbul: Okeanos- Foundation for the Sea.
- Hermannsen, L., Mikkelsen, L., Tougaard, J., Beedholm, K., Johnson, M., & Madsen, P. T. (2019). Recreational vessels without Automatic Identification System (AIS) dominate anthropogenic noise contributions to shallow water soundscape. *Scientific Report Nature Reseach*. doi:<https://doi.org/10.1038/s41598-019-51222-9>
- Hunt, F. V. (1954). *Electroacoustic: The analysis of transduction, and its Historical Background*. New York: Harvard Univ Press / John Wiley.
- IMO. (1973). *International Convention for the Prevention of Pollution from Ships*. IMO.
- IMO. (1974). *International convention for the Safety of Life at Sea (SOLAS)*. International Maritime Organization.

- Kell, G. S. (1970). Isothermal compressibility of liquid water at 1 atm. *Americal Chemical Society*, 119-122.
- Kinsler, L. E., Frey, A. R., Coppens, A. B., Sanders, J. V., , & . (2011). *Fundamentos de Acústica*. México DF: Limusa.
- Kumar Mahapatra, R. (2017). *Received Signal Strength based localization in Wireless Sensor Network*. Surathkal.
- Mackenzie, K. V. (1981). Nine-term equation for sound speed in the oceans. *The journal of the Acoustical Society of America*, 807.
- Marine Traffic. (n.d.). *marinetraffic*. Retrieved June 15, 2022, from <https://help.marinetraffic.com/hc/en-us/articles/204581828-What-is-the-Automatic-Identification-System-AIS->
- McCarthy, E. (2004). *INTERNATIONAL REGULATION OF UNDERWATER SOUND*. Boston: KLUWER ACADEMIC.
- McKenna, M., Ross, D., Wiggins, S., Hildebrand, J., , & . (2012). Underwater radiated noise from modern commercial ships. *The Journal of the Acoustical Society of America*, 92-103.
- Monzingo, R. A., & Miller, T. W. (1980). *Introduction to Adaptive Arrays*. New York: Wiley.
- Nations, U. (2022, June 15). *United Nations Environment Programme*. Retrieved from [unep.org](http://unep.org)
- Nehorai, A., & Paldi, E. (1994). Acoustic vector-sensor array processing. *Signal processing, IEEE Transactions*, 2481-2491.
- OECD. (2022, May 13). *Organization for Economic Co-operation and Development*. Retrieved from [oecd.org](http://oecd.org)
- Pohlmann, K. C., & Everest, F. A. (2009). *Master Handbook of Acoustics* (Fifth ed.). New York: McGraw-Hill.
- Pourmohammad, A., & Mohammad, S. (2013). N-dimensional N-microphones sound source localization. *EURASIP Journal on Audio, Speech, and Music Processing*, 27.
- Ralston, A., & Rabinowitz, P. (1978). *A First Course in Numerical Analysis*. New York: Dover Publications.
- Ross, D. (1922). *Mechanics of Underwater Noise*. Pasadena, California: Pergamon Press Inc.
- Santos-Domínguez, D., Torres-Guijarro, S., Cardenal-López, A., Pena-Gimenez, A., , & . (2016). ShipsEar: An underwater vessel noise database. *Applied Acoustics*, 64-69.
- Shannon, C. E. (1949). Communication in the Presence of Noise. *Proceedings of the IRE*, 10-21. doi:<https://doi.org/10.1109/jrproc.1949.232969>
- Sullivan, E. J. (2015). *Model-Based Processing for Underwater Acoustic Arrays*. Portsmouth: Springer.



- Tesei, A., Fioravanti, S., Grandi, V., Guerrini, P., Maguer, A., & . (2010). ACOUSTIC DETECTION OF SMALL- AND MID-SIZED SURFACE VESSELS IN VERY SHALLOW WATERS. *NATO Undersea Research Centre*,.
- Tessei, A., Fiovaranti, V., Guerrini, P., Marquer, A., , & . (2011). *Acoustic surveillance of small boats in confined areas*. SYMPOL 2011.
- UN. (1982). *United Nations Convention on the Law of the Sea*. UN.
- Wittekind, D. K. (2017). *Ship Acoustics - Basic (Lecture slides)*. DW ShipConsult.
- Wittekind, D. K. (2017). *Ship Acoustics - Underwater Noise (Lecture Slides)*. DW ShipConsult.
- Wittekind, D. K. (2017). *Ship Acoustics -Propeller Noise (Lectures slides)* . DW ShipConsult.
- Xerri, B., Cavassilas, F., Borloz, B., , , & . (2000). Passive tracking in underwater acoustic. *Signal processing*, 1067-1085.
- Xunxue, C., Kegen, Y., Songsheng , L., , , & . (2018). Approximate Closed-Form TDOA-Based Estimator for Acoustic Direction Finding via Constrained Optimization. *IEEE Sensors*, 3360-3371.